Instituto Superior de Engenharia de Lisboa
Área Departamental de Engenharia Mecânica

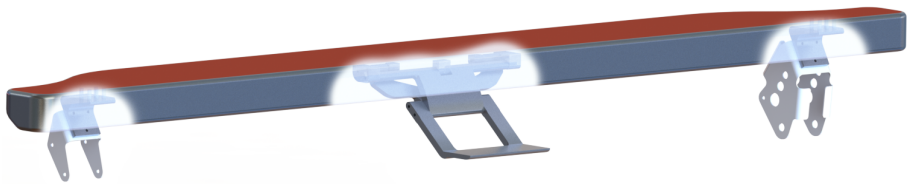

Design of a Boarding Step for a Helicopter

Rafael De Gomes Monteiro

Bachelor in Mechanical Engineering

A thesis submitted in fulfilment of the requirements for
the degree of Master in Mechanical Engineering

Advisers:
PhD João de Almeida Milho
MSc Afonso de Sousa Leite

Co-Advisers:
MSc Ingo Rohacek-Costa
MSc Stefan Harms

Jury Panel:
President: PhD Vitor Manuel Rodrigues Anes
Vowels: PhD Ricardo José Fontes Portal
PhD João Filipe de Almeida Milho

December 2018

This page is intentionally left blank

Instituto Superior de Engenharia de Lisboa
Área Departamental de Engenharia Mecânica

Design of a Boarding Step for a Helicopter

Rafael De Gomes Monteiro

Bachelor in Mechanical Engineering

A thesis submitted in fulfilment of the requirements for
the degree of Master in Mechanical Engineering

Advisers:
PhD João de Almeida Milho
MSc Afonso de Sousa Leite

Co-Advisers:
MSc Ingo Rohacek-Costa
MSc Stefan Harms

Jury Panel:
President: PhD Vitor Manuel Rodrigues Anes
Vowels: PhD Ricardo José Fontes Portal
PhD João Filipe de Almeida Milho

December 2018

This page is intentionally left blank

À mãe e ao pai pelo apoio incondicional,
aos amigos pelos momentos de lazer,
aos orientadores pelos ensinamentos,
à Beatriz pelo apoio emocional inabalável,
A todos, um enorme obrigado.

This page is intentionally left blank

Resumo

O presente trabalho foi elaborado em parceria com a Airbus Helicopters Deutschland GmbH (AHD) e o Instituto Superior de Engenharia de Lisboa (ISEL) como um Trabalho Final de Mestrado e consiste no desenvolvimento de um Degrau de Embarque (Boarding Step) para um helicóptero.

É uma abordagem à fase inicial de desenvolvimento de um equipamento externo para helicópteros de pequeno e médio porte tendo em vista a futura certificação aeronáutica.

O processo de desenvolvimento passa por várias etapas de *brain-storming* e modelação até ser obtido um modelo com características apelativas e funcionais. Após obtenção do modelo realiza-se o desenvolvimento de um degrau adicional que facilita o embarque para utilizadores de mobilidade reduzida.

Posteriormente realizou-se o estudo estático e dimensionamento estrutural dos componentes respondendo às especificações da indústria.

No fim do presente trabalho encontra-se desenvolvido um degrau de embarque que inclui um degrau adicional extensível. São apresentados três modelos viáveis, dois em liga metálica e um em compósito, que servem de base para futuro desenvolvimento pela empresa.

Abstract

The present work was developed in partnership with AHD and ISEL as a Master of Science Thesis and consists of Designing a Boarding Step for a helicopter.

It is an approach to the initial development of an outboard equipment for small and medium helicopters with aim for aeronautical certification.

The design process begins via brain-storming and modelling until a valid model is obtained with appealing and functional characteristics. Afterwards begins the development of an additional swivel step which aims to ease boarding for users with reduced mobility.

In a later stage, static analysis and dimensioning of the components was performed, all the while with respect to the industry's specifications.

At the end of the work, a boarding step with an additional retractable step is developed. Three viable models are presented, two in metallic alloy and another in composite materials, which will serve as a basis for future development by the company.

Palavras-Chave

Degrau de embarque, Equipamento Externo de Helicópteros, Design, Certificação Aeronáutica, Método de Elementos Finitos, Análise de Elementos Finitos

Keywords

Boarding step, Outboard Helicopter Equipment, Design, Aeronautical Specification, Finite Element Method, Finite Element Analysis

This page is intentionally left blank

Glossary

AHD	Airbus Helicopters Deutschland GmbH
Add Step	Additional Step
Board Step	Boarding Step
CAD	Computer-Aided Design
CATIA	CATIA V5-6R 2017 by Dassault Systèmes
CS	Certification Specification
CFUD	Unidirectional Carbon Fibre
CH	Centred Holes
DoF	Degrees of Freedom
EASA	European Aviation Safety Agency
FEA	Finite Element Analysis
FEM	Finite Element Method
FoS	Factor of Safety
IBS	Inner Building Stairs
IRT	Increased Rear Tab
ISEL	Instituto Superior de Engenharia de Lisboa
F2U	Floats 2 Ultimate Combined Loads Load Case
LED	Light Emitting Diode
SW	SolidWorks 2017 by Dassault Systèmes
VARTM	Vacuum Assisted Resin Transfer Molding
VIP	Very Important Person

Symbols

2D	Two-Dimensional, defaults to XoY Plane
3D	Three-Dimensional
A_p	Section Area of Pin
F_{CD}	Direct Shear Force
F_{CI}	Indirect Shear Force
F_{CT}	Total Shear Force
h	Rise
HC	Hand-Calculated Value
l,a	Width
l_x	Distance from applied force to location x
l_{xy}	Distance from x to y
lg_{xy}	Distance from applied force to geometric centre between x and y
N_{SP}	Number of Shear Pins
SW	Result of a simulation done in SolidWorks
u	Undercut
U	Elastic Strain Energy of a System
w	Tread
$w_{x,y}$	Deflection or Deformation
Π	Total Potential Energy of a System
$\boldsymbol{\delta}_{\max}$	Maximum Displacement
$\boldsymbol{\sigma}_{\max}$	Maximum Stress
$\boldsymbol{\sigma}_{ys}$	Yield Stress (Elastic Limit)
$\boldsymbol{\tau}_{ADM}$	Allowable Shear Pressure
$\boldsymbol{\tau}_{op}$	Operating Shear Pressure
$\boldsymbol{\phi}_{ph}$	Pin-hole Diameter
Ω	Work done by lateral surface loading $p(x, y)$

Contents

List of Figures

List of Tables

Chapter 1

Introduction

The present work was developed in partnership with ISEL and AHD as a Master of Science Thesis and consists of Designing a Boarding Step for AHD.

The current chapter will synthesize as best as possible and with the utmost clarity the information throughout the work, enabling the reader to understand the methodology and sequencing taken into account during its development.

1.1 Functional Framework

Existing models of civil helicopters such as the H145 (Figure 1.1) ship with the standard landing gear which includes a sidebar to aid boarding. When a helicopter is in use, the boarding procedure consists of climbing two steps of approximately equal height, around 400 mm apart.

In order to combat this, a Boarding Step (Board Step) will be developed in order to provide handicapped and/or Very Important Person (VIP) customers a more pleasant and easier boarding experience. A meeting was held in mid October 2017 to begin the brainstorming process as well as define the needs that the design had to meet in order to be useful and fulfil the roles it was intended for.

1.2 Objectives

The first meeting established the foundations and objectives that needed fulfilling. These eventually changed slightly to accommodate the results of the brainstorming process (described in Section 3.1) and are as follows:

- Design a Board Step to aid boarding into AHD Helicopters;

Figure 1.1: Model H145 with highlighted boarding sidebar
Adapted from Airbus' website

- Model the Board Step and the Additional Step (Add Step) in 3D modelling software;
- Perform Static Analysis guided by documents provided by AHD and European Aviation Safety Agency (EASA)s' CS 27 & 29;
- Choose the correct metallic connections and calculate their necessary dimensions;
- Improve upon the parts of the modelled assembly by optimizing stiffness to weight ratio.

Other than the previously mentioned objectives there are a few smaller additions such as choosing an anti-skid surface to coat the top of each step, including a Light Emitting Diode (LED) as a visual aid and other overall improvements to functionality and manufacturability. These along with other ideas are listed in Chapter 6.

1.3 Planning and Execution

The planning proposal was submitted in early October 2017 by the student and then reworked with input from the advisers in order to contain all objectives in a time framework that allocates enough time to each task. This planning proposal is visible in Appendix A.

The first four months were mostly allocated to know-how gathering and defining the objectives that needed to be met. In these first few months several design options were considered, some of which were modelled (as can be seen in Section 3.1), with the goal to achieve a practical yet simple design. The first designs were meant to be simple add-ons to the current tubular structure of the aircrafts with the reason being to limit the amount

of added weight. Section 3.1 describes more in depth the brainstorming process as well as provides illustration of some of the first sketched ideas.

From early February to mid-April 2018 the goal was to finish the Preliminary Concept Design which meant selecting the final design and having it modelled. From then on there were no major changes to the overall assembly or parts as far as functionality and application are concerned. This was fulfilled by the end of January 2018, with a month in advance, soon after a meeting with AHD in which some criteria was provided as a must-have for this new equipment. With the opportunity to fully replace the Board Step, this meant the design could evolve to include an additional swivel-step aptly named Add Step. Section 3.2 thoroughly describes the reasoning behind adding the Add Step as well as its design process and challenges. The full prototype model was finished mid-way through February 2018 and is visible in Figure 3.12.

At the end of April 2018 the plan was to start the Detailed Concept Design which would add finishing touches to the models and start the Static Analysis (detailed in Chapter 4). From then onward the planning comprised of improving the design as well as finishing writing. Instead, the analysis stage began in March 2018, when the first analytical calculations brought to light some design flaws in the arm and leg links. These were then redesigned and went through several Finite Element Method (FEM) iterations and remodelling until the desired result was obtained (visible in Figures 4.11 and 4.15). The analysis of the Board Step followed suit and its model was also subject to numerous changes.

By the end of this project, a working prototype with the basis for certification in the aeronautical industry was developed. This prototype is comprised of eight (8) parts, seven (7) of which unique, five (5) designed by the student. The prototype also has a working dynamic sub-system which is comprised of the arm and leg links as well as the Add Step. This sub-system allows the Add Step to extend when in use and retract back to a hidden storage-state when not in use.

Chapter 2

Theoretical Framework

The current chapter aims to describe the methodology employed throughout the work.

2.1 Specifications

2.1.1 EASA CS 27 & 29

The EASA regulates, as the name suggests, the safety regarding all aviation vehicles, equipment and systems. This project has to abide to the Certification Specification (CS) for Small Rotorcrafts and the CS for Large Rotorcrafts alike seeing as how its development is linked to rotorcrafts of both these size categories. Each of these CS is composed of two (2) books: the Airworthiness Code and the Acceptable Means of Compliance. For the applications required by this project only the Airworthiness Code will be consulted, specifically Sub-parts C – Strength Requirements and D – Design and Construction.

AHD specified two sets of focal points, the first one guided the brainstorming process (refer to Section 3.1):

- 601 Design;
- 603 Materials;
- 605 Fabrication methods;
- 609 Protection of structure;
- 610 Lightning and static electricity protection;
- 611 Inspection provisions.

The second paired with the AHD Requirements Specification to instruct the requirements of static analysis:

- 301 Loads;
- 303 Factor of Safety (FoS);
- 305 Strength and deformation;
- 307 Proof of structure;
- 337 Limit manoeuvring load factor;
- 501 Ground loading conditions: landing gear with skids;
- 521 Float landing conditions;
- 563 Structural ditching provisions;
- 613 Material strength properties and design values;
- 625 Special factors.

Following these guidelines is paramount to the industry seeing as how they increase the occupants and operators' chances of survival dramatically in a number of catastrophic events. As an example, item 521 of both CS 27 and CS 29 "introduces a new flotation stability certification methodology that takes into account sea conditions for which certification is requested" [1].

Item 601 states "The rotorcraft may have no design features (...) that experience has shown to be hazardous (...)." [2, 3]. Not only that but any design feature such as a Board Step which is intended to increase occupants comfort must be designed to be reliable enough that it would not hamper helicopter missions or physically interfere with other already installed systems or equipment. For the Board Step this also includes resistance to weathering, corrosion and abrasion as well as having low enough mass that it would be viable to be installed on both sides of the helicopter without hindering manoeuvrability.

2.1.2 Airbus Helicopters Deutschland Requirements Specifications

The loads divide into limit and ultimate loads and are defined by AHD. Limit loads include a load safety factor and represent the minimum loads the device should withstand during a specific scenario without plastic deformation. Ultimate loads also include a load safety factor (slightly higher) and represent the minimum loads above which the device is allowed to and should break (Figure 2.1). If the device withstands loads much higher than the

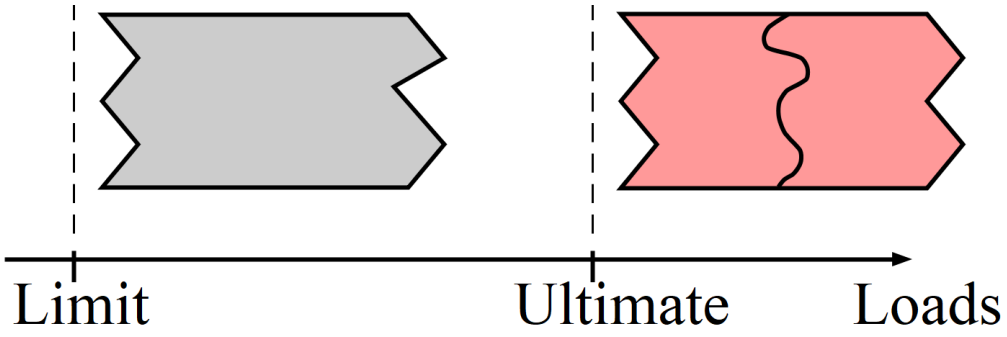

Figure 2.1: Visual representation of the definition of limit and ultimate loads

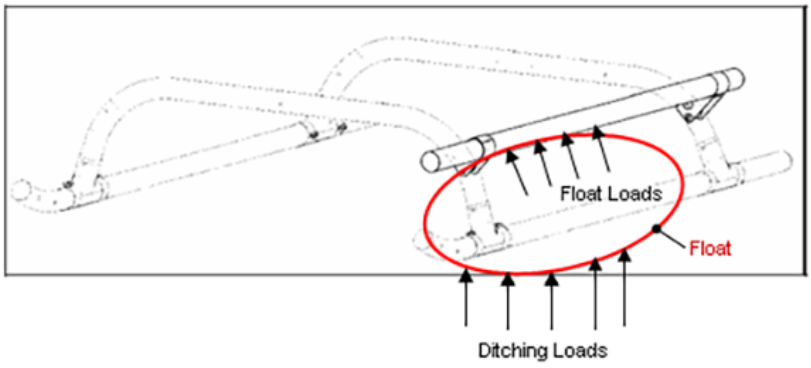

Figure 2.2: Ditching Loads and Float Loads
Source: AHD's Requirements Specification

defined ultimate load, for a specific scenario, then its design should be reassessed because its over-dimensioned. There's also mention of emergency landing and manoeuvring load factors which are represented in multiples of the acceleration of gravity – ex.: $2g = 2 \cdot 9.81 \text{m/s}^2$. These are applied independently, that means without combination in any of the given directions: Upward, Downward, Aft ward, Forward, Sidewards.

CS 27/29.521 refers to water landings, in this scenario it's important to consider the loads applied on the step by the external float system. If the helicopter ditches onto the water with fully immersed floats, these will push against the step (Figure 2.2). This scenario considers multiple load cases which combine differing load values in all three (3) axis.

The step must also be tested for its intended application, which is to carry three (3) persons. Their load is to be applied as visible in Figure 2.3. In these calculations, the step's own weight is to be considered and it must work normally under this condition as well as not suffer damaged from it.

In the course of the bi-weekly meetings, a request came through that comprised of a question that is to be only partially answered in this project. The request asked specifically what would be the mass and displacement discrepancy between the Board Step made out of

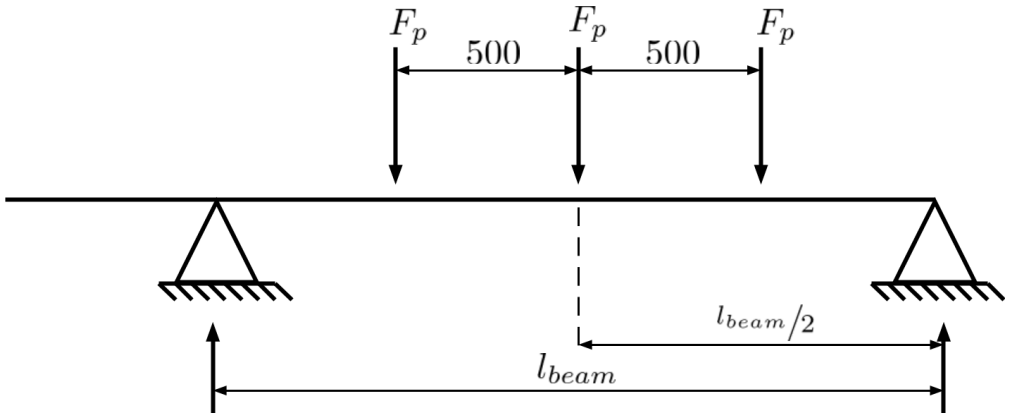

Figure 2.3: Three (3) persons load atop the Step

aluminium and the same design (with necessary changes) made out of composite materials – namely a carbon fibre and honeycomb sandwich. What is requested is essentially to compare if the weight difference (expected to be lower for the composite) is worth the investment in manufacturing via Vacuum Assisted Resin Transfer Molding (VARTM) or Automated Layup. This composite study is only partial because it's outside the original scope of the project.

2.2 Structural Design

2.2.1 Analytical Calculations

2.2.1.1 Universal Equations Method for Determining Elastic Curve on Beams

It's possible to attain the reaction forces of a given 2D problem using the three (3) Static Equilibrium Equations so long as its constraints amount to no more than three (3) unknown variables. If however determining the displacement of one or more points is an objective then an equation that approximates the beam's displacement is needed. Determining the curvature at various points of a beam allows the definition of the *elastic curve* which aids in ascertaining a beams behaviour when subjected to loads. In the case of statically determinate beams it's easy to apply the method of superposition to tabled formulas, yielding the deflection and slopes for various loadings and types of support. The principle of superposition states that the effect of a given combined load on a structure can be obtained by applying the various loads separately and combining the results, provided the following conditions are satisfied:

1. Each effect is linearly related to the load that produces it;

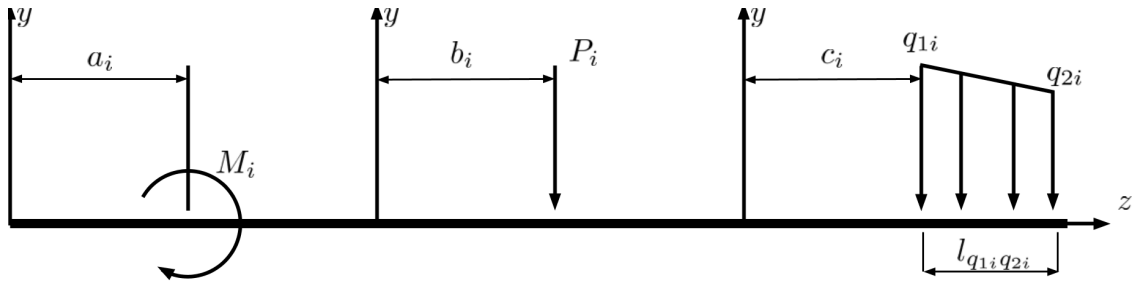

Figure 2.4: Illustration of symbols represented in Equation (2.1)

2. The deformation resulting from any given load is small enough not to affect the conditions of application of the other loads.

The Universal Equations method performs the same task including respecting the principle of superposition all the while being easier to apply to statically indeterminate beams (with two (2) or more supports). Equations (2.1a) and (2.1b) return the deformation and slope respectively of any loaded beam with respect to $EIy \mid EI\theta$ making it possible to obtain the elastic curve $y_{(x)}$ by dividing the result by the intended beam's geometric and material properties (namely the Moment of Inertia and Young's Modulus). The universal equations' variables are illustrated in Figure 2.4 but more complex scenarios can also be modelled by combining its elements.

$$EIy = EIy_0 + EI\theta_0\, z + \sum_{i=1}^{n} M_i \frac{(z-a_i)^2}{2!} + \sum_{i=1}^{m} P_i \frac{(z-b_i)^3}{3!} + \\ + \sum_{i=1}^{k} \left(q_{1i} \frac{(z-c_i)^4}{4!} + \frac{q_{2i} - q_{1i}}{l\, q_{1i}\, q_{2i}} \frac{(z-c_i)^5}{5!} \right) \tag{2.1a}$$

$$EI\theta = EI\theta_0 + \sum_{i=1}^{n} M_i (z-a_i) + \sum_{i=1}^{m} P_i \frac{(z-b_i)^2}{2!} + \\ + \sum_{i=1}^{k} \left(q_{1i} \frac{(z-c_i)^3}{3!} + \frac{q_{2i} - q1i}{l\, q_{1i}\, q2i} \frac{(z-c_i)^4}{4!} \right) \tag{2.1b}$$

2.2.1.2 Rayleigh-Ritz Method for Classic Thin Plates Theory

Plates are defined as structural elements limited by two (2) plane surfaces that are distanced from each other an interval denominated as thickness. It's possible to distinguish between three kinds of plates: (1) thin plates with small deflections, (2) thin plates with large deflections, (3) thick plates. For the purpose of this project only the first two are significant and the classic theory of thin plates with small deflections is applicable. This theory makes the following assumptions [5, 6, 7]:

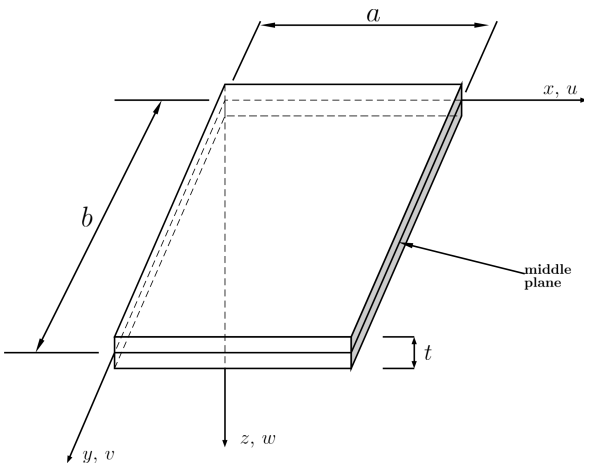

Figure 2.5: Representation of a thin plate and its middle plane

- The plate is elastic, homogeneous and isotropic;
- There is no deformation in the mid-plane of the plate (Figure 2.5). This plane remains unstrained subsequent to bending;
- The thickness of the plate is very small in comparison with the other dimensions ($t \approx 1/20\, a \wedge 1/20\, b$);
- The deflections of the plate are small in comparison with its thickness ($w < t$). The slope of the deflected surface is therefore very small and the square of the slope is a negligible quantity in comparison with unity;
- Deflections occur such that planes normal to the mid-plane remain perpendicular after bending – this means the vertical shear strains $\gamma_{xz} = \gamma_{yz} = 0$;
- Stress normal to the mid-plane is irrelevant when compared to the other two main stresses $\sigma_{33} << \{\sigma_{11}, \sigma 22\} \therefore \sigma_{33} \approx 0$.

The so-called Ritz method or Rayleigh-Ritz method is a convenient procedure for determining solutions that would otherwise be too difficult (or impossible) to achieve analytically via the principle of minimum potential energy. It's based off of the theoretical principals of Euler and Bernoulli and is applicable to beams (finding the approximate real resonant frequencies of systems with more than one Degrees of Freedom (DoF)) as well as plates. In the case of plates, the first procedure is to choose two (2) equations (one for each axis) such as φ in the form of a series containing undetermined parameters $a = C_{mn}$ $(m, n = 1, 2, \ldots)$ that must satisfy the geometric boundary conditions.

Afterwards it's possible to define the displacement approximation Equation (2.2).

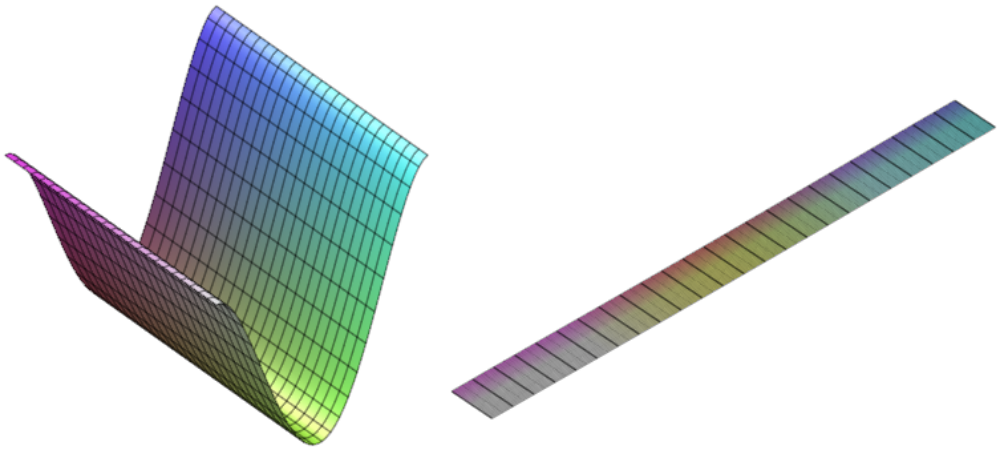

Figure 2.6: Example displacement plots of a plate achieved by the Rayleigh-Ritz Method

$$w_{(x,y)} = \sum_{j=1}^{J} C_j \cdot \Phi_j(x,y) = \sum_{m}^{M} \sum_{n}^{N} C_{mn} \cdot \varphi_m(x) \cdot \varphi_n(y) \tag{2.2}$$

This equation is the used to represent the Elastic Strain Energy U as:

$$U = \frac{1}{2} \iint_A D \left\{ \left(\frac{\partial^2 w}{\partial x^2} + \frac{\partial^2 w}{\partial y^2} \right)^2 - 2(1-\nu) \left[\frac{\partial^2 w}{\partial x^2} \frac{\partial^2 w}{\partial y^2} - \left(\frac{\partial^2 w}{\partial x \partial y} \right)^2 \right] \right\} \mathrm{dA} \tag{2.3}$$

Equation (2.4) represents the work done by the lateral surface loading $p(x,\, y)$.

$$\Omega = - \iint_A p_z w_{(x,y)} \ \mathrm{dA} \tag{2.4}$$

Therefore, the potential energy is $\Pi = U + \Omega$. It is now possible to determine the values of all C_{mn} by using the Rayleigh quotient to obtain all the eigenvalues. After the values are obtained, the displacement approximation function w is fully defined and can be plotted in 3D form as shown in Figure 2.6

Orthotropic Materials

If however the plate's material properties are not the same in all axis - orthotropic material - the equation for the Elastic Strain Energy U is slightly different and is represented like so:

$$U = \frac{1}{2} \iint_A D_{11} \cdot \kappa_x^2 + D_{22} \cdot \kappa_y^2 + 2 \cdot D_{12} \cdot \kappa_x \kappa_y + 4 \cdot \kappa_{xy} \left(D_{13} \cdot \kappa_x + D_{23} \cdot \kappa_y + D_{33} \cdot \kappa_{xy} \right) \mathrm{dA} \tag{2.5}$$

Where the κ_x, κ_y, κ_{xy} represent $\frac{\partial^2 w_{xy}}{\partial x^2}$, $\frac{\partial^2 w_{xy}}{\partial y^2}$, $\frac{\partial^2 w_{xy}}{\partial x \partial y}$ respectively and the D matrix is the Bending Stiffness Matrix of the laminate.

The D matrix is obtained by adding the different D_k matrices, where k represents each ply.

Each D_k is obtained from the Transformed Reduced Elastic Coeficient Matrix for each ply $\bar{Q}_k$ which themselves are obtained from the Reduced Elastic Coefficient Matrix of the laminate Q. These are written below as such:

$$D_{ij,\,k} = \frac{1}{3} \cdot \bar{Q}_{ij,\,k} \cdot \left(z_k^3 - z_{k-1}^3\right) \ , \ \text{where } z_k \equiv \text{Thickness of Layer k} \tag{2.6}$$

$$Q = \begin{bmatrix} \dfrac{E_x}{1 - \nu_{xy} \cdot \nu_{yx}} & \dfrac{\nu_{xy} \cdot E_y}{1 - \nu_{xy} \cdot \nu_{yx}} & 0 \\ \dfrac{\nu_{xy} \cdot E_y}{1 - \nu_{xy} \cdot \nu_{yx}} & \dfrac{E_y}{1 - \nu_{xy} \cdot \nu_{xy}} & 0 \\ 0 & 0 & G_{xy} \end{bmatrix} \tag{2.7}$$

$$\bar{Q} = \begin{bmatrix} \bar{Q}_{11} & \bar{Q}_{12} & 0 \\ \bar{Q}_{21} & \bar{Q}_{22} & 0 \\ 0 & 0 & \bar{Q}_{66} \end{bmatrix} \tag{2.8}$$

Where the entries for $\bar{Q}$ are for each layer k:

$$\begin{aligned}
\bar{Q}_{11} &= Q_{11} \cdot \cos^4(\theta_k) + 2 \cdot (Q_{12} + 2 \cdot Q_{66}) \cdot \sin^2(\theta_k) \cdot \cos^2(\theta_k) + Q_{22} \cdot \sin^4(\theta_k) \\
\bar{Q}_{12} &= (Q_{11} + Q_{22} - 4 \cdot Q_{66}) \cdot \sin^2(\theta_k) \cdot \cos^2(\theta_k) + Q_{12} \cdot (\sin^4(\theta_k) + \cos^4(\theta_k)) \\
\bar{Q}_{22} &= Q_{11} \sin^4(\theta_k) + 2 \cdot (Q_{12} + 2 \cdot Q_{66}) \cdot \sin^2(\theta_k) \cdot \cos^2(\theta_k) + Q_{22} \cdot \cos^4(\theta_k) \\
\bar{Q}_{16} &= (Q_{11} - Q_{12} - 2 \cdot Q_{66}) \cdot \sin(\theta_k) \cdot \cos^3(\theta_k) + (Q_{12} - Q_{22} + 2 \cdot Q_{66}) \cdot \sin^3(\theta_k) \cdot \cos(\theta_k) \\
\bar{Q}_{26} &= (Q_{11} - Q_{12} - 2 \cdot Q_{66}) \cdot \sin^3(\theta_k) \cdot \cos(\theta_k) + (Q_{12} - Q_{22} + 2 \cdot Q_{66}) \cdot \sin(\theta_k) \cdot \cos^3(\theta_k) \\
\bar{Q}_{66} &= (Q_{11} + Q_{22} - 2 \cdot Q_{12} - 2 \cdot Q_{66}) \cdot \sin^2(\theta_k) \cdot \cos^2(\theta_k) + Q_{66} \cdot (\sin^4(\theta_k) + \cos^4(\theta_k))
\end{aligned} \tag{2.9}$$

2.2.2 Finite Element Method

FEM is currently widely used to solve structural and fluid problems in industrial applications. When using the FEM, computer code assists in assembling and solving large systems of algebraic equations. These pre- and post-processing tools are integrated into Computer-Aided Design (CAD) software such as SolidWorks 2017 by Dassault Systèmes (SW) or CATIA V5-6R 2017 by Dassault Systèmes (CATIA). In order to implement FEM to a particular design, one needs to divide its model into several small pieces of simple shapes called elements which band together into a mesh effectively taking the models place and replacing a complex problem with many simple ones that need to be solved simultaneously [8, 9, 10].

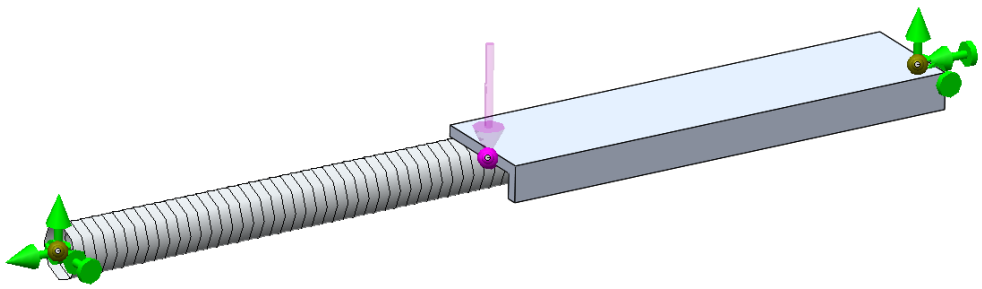

Figure 2.7: Example of Mesh and Loads on a beam element in SolidWorks

An important feature is that the elements do not leave gaps between each other or overlap geometrically but together fill the entirety of the volume of a solid or fluid. The application of FEM allows for the material properties to be non-homogenous (dependent on location) and/or anisotropic (dependent on direction). Analysis achieved via the FEM is aptly named Finite Element Analysis (FEA) and in SW static analysis studies essentially calculate displacements, reaction forces, strains, stresses, failure criterion, FoS and error estimates [8, 11].

2.2.2.1 Beam, Shell and Solid Elements

The three main structural components used in 3D CAD are Beams, Shells and Solids. When it comes to their use in software, beams are defined as being able to resist bending, shear and torsional loads. Figure 2.7 is a visual representation of what a beam looks like in SW's Static Analysis Module. In order to extrude a beam element, the program requires the exact cross section so it is able to calculate the moments of inertia, neutral axes and the distances from the extreme fibers to the neutral axes. Also visible in Figure 2.7 are joints (in green at the ends, in purple in the middle) which allow intersection of several structural members and also allow the application of external forces or reactions. Each joint is assigned six (6) DoF and the program allows the prescription of zero or non-zero translations and rotations.

In studies with beams, shell and solid surfaces it is possible to bond beams or their joints to solid and shell faces. This decreases the computation load as it eliminates the need to compute contact between structural elements. As for meshing beams, there are a few settings and they include differing the amount of elements or element size on a selected beam.

Shell elements are 2D elements with no thickness which are capable of resisting membrane and bending loads. SW generates one of the types of elements shown in Figure 2.8: linear triangular shell elements with 3 nodes for a draft quality mesh – these are a good way of getting preliminary results with less time – and parabolic triangular shell elements with 6 nodes for a high quality mesh – these are more precise but also include twice as many nodes

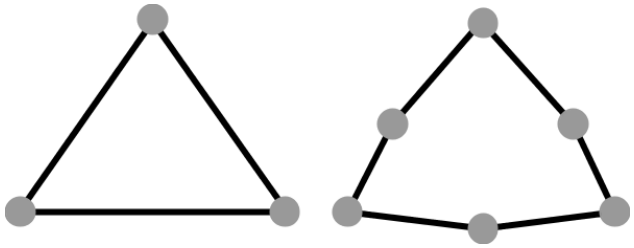

Figure 2.8: Linear triangular and parabolic triangular shell mesh elements

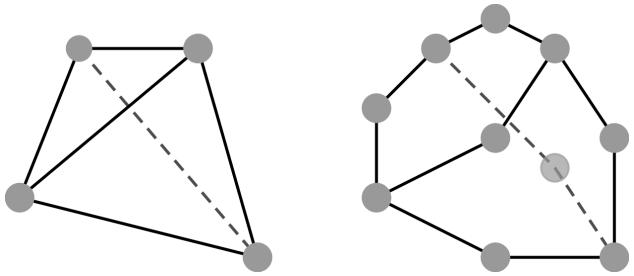

Figure 2.9: Linear tetrahedral and parabolic tetrahedral solid mesh elements

which in turn increase the requirement for computation power and time taken to finish the analysis.

Shells are generated from surfaces which can be simple (Ex.: plate, bed cover of a pickup truck) or complex (Ex.: car bodywork, motorcycle fairing). For structural studies, each node in the shell mesh elements has six (6) DoF – translation in and rotation about all three (3) axis. When meshing, the software allows the input of element size and element growth ratio (factor of longest over shortest element in a part).

For solid elements, SW generates one of the types of elements shown in Figure 2.9: linear tetrahedral solid elements with 4 nodes for a draft quality mesh – same as the shell draft, these are good for preliminary results with low impact on computation time – and parabolic tetrahedral solid elements with 10 nodes for a high quality mesh – these more accurately determine curved boundaries and also produce better mathematical approximations at the cost of greater computational resources than linear elements.

Solid meshes can be generated from any solid geometry, from a simple cube to a twisted torus. For structural studies, each node in a solid mesh contains three (3) DoF which represent the translations in all three (3) orthogonal directions.

2.2.3 Metallic Connections

Metallic connections can be considered a sub-group of the larger elementary methods of fastening. They contain bolts, nuts, cap screws, set-screws, rivets, spring retainers, pins, keys, welds and locking devices. Studies in this field often yield instructions on various

joining methods as well as simplifications applicable to several problems. When it comes to sizing metallic connections, the EN 1993-1-8 [12] and EN 1999-1-8 [13] provide a good thorough basis for the basic calculations. The calculations for pins in Section 4.2.5 were based on Shigley's Mechanical Engineering Design [14] with emphasis on the good practices mentioned in the Eurocodes [12, 13].

The current design for manufacturing has a very strict goal to decrease as much as possible the quantity of connections within a project to not only increase reliability but also to keep costs low.

2.3 Ergonomics of Climbing Steps

In *Kodak's Ergonomic Design for People at Work*, Staff and Company [15] define six (6) steps for an ergonomics problem-solving technique. Some of these go without saying while others provide useful information as to which parameters to look for when designing, such as risks - standing on uneven or slippery surfaces - or the mindset behind generating solutions for these problems.

Neufert and Neufert [16] reference in their book - *Architects' Data* - that the recommended height between steps (henceforth referred to as *rise*) should be at a 17/29 ratio to the perceived depth of the steps (henceforth referred to as *tread*). This means that for a rise of 400 mm, the tread would ideally be $400 \cdot {}^{29}/_{17} \approx 682$ mm, which is unfeasible. Not only would the tread be too large to fit in a Helicopter's assembly, but a rise of 400 mm is extremely uncomfortable. Its worth noting that this ratio is described as being ideal for Inner Building Stairs (IBS) and that for extreme values (be they low or high) there is no general rule to follow.

Further, in [17, Table D-1] for an angle to horizontal of $\approx 50\,^{\circ}$ it is recommended to have a rise of ≈ 24 cm and a tread of $\approx 20,5$ cm.

The authors of [15, 17, 18] agree that a slope of of 50° is suitable for what is referred to as Stair-Ladders. Furthermore, [17] states that as the slope increases, so should the rise (up to a value of 24 cm) while the tread should decrease.

In an attempt to better understand the measurements of stairs used in everyday life, several IBS were measured and their values for rise (h), tread (w), width (l) and undercut (u) can be viewed in Table 2.1. Along with taken measurements is the ideal stair ratio as defined by Neufert and Neufert [16, pg. 191-195].

The ratio referred previously reflects the average rise of 170 mm as can be seen in Table 2.1. There's also mention that the sum of two rises and one tread should equal the stride of an adult on a horizontal plane ($2h + w \approx 62.5$ mm).

In their study on knee surgery patients, Murakami et al. [19] got a rating of 3.7/5 for climbing 200 mm stairs in their postoperative clinical data which leads to believe that al-

Table 2.1: Measurements of several building stairs

	w (mm)	l (mm)	h (mm)	u (mm)
Ideal	290	500	170	30
IBS#1	260	1220	170	25
IBS#2	270	920	185	25
IBS#3	320	890	195	45
IBS#4	260	880	165	50

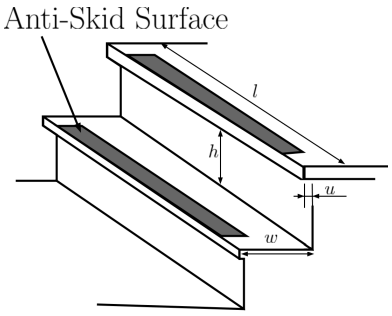

Figure 2.10: Representation of anti-skid surface on a stairway
Adapted from Staff and Company

though the ideal rise is 170 mm, a slightly larger vertical gap is still a viable and comfortable alternative.

There seems to also be a consensus when it comes to having an anti-skid surface on the tread. Whether that comes from the material itself or a coating is a matter of design choice. An anti-skid surface will also be more easily visible by having a higher contrast to its surroundings than the remainder of the step (Figure 2.10). For this topic there are some key points in literature:

- Anti-skid should have strong contrast be of a different hue to the rest of the tread therefore making it easily distinguishable;
- The whole tread should have matte finish to prevent indirect or reflective glare from daylight or overhead lighting;
- When designing for outdoor usage, there should be additional lighting to aid visibility.

Chapter 3

Design of the Boarding Step

The current chapter covers all the modelling work, that was carried out in order to fully design the Board Step, Add Step and all its component parts.

3.1 Early Brainstorming and Various Models

In this first brainstorming stage, several possibilities were taken into account and scribbled down. Some were just sketched ideas while others were modelled with the possibility of being used later on.

The idea at first was to simply add steps to the existing landing gear in order to reduce the rise - distance between two steps in stairs - which would ease boarding. The designs in Figures 3.1d and 3.1e stem from that plan while Figures 3.1a to 3.1c are more elaborate ideas that include dynamic mechanisms aimed at increasing step count.

Figure 3.1d shows a red top surface which represents an anti-skid surface along with a protection bar at the end of the step providing some restraint so the users' feet wouldn't go past the step, ending in injury. It also included a chamfer in the beginning of the top face which ended up being scrapped since it wouldn't be beneficial. This design would help mitigate the rise between the landing gear and the helicopter flooring but would end up making it harder for someone with difficulties to reach the first Add Step as it would effectively remove the utility of the landing gear as a step.

Figure 3.1e was designed with the objective of being just a single part with the possibility of being used both above and below the landing gear effectively mitigating the difference in height between the ground and the landing gear. Not only that but by being skewed off to the side, this part allows the use of the landing gear as a step reducing even further the rise between each.

During a meeting midway through October 2017 the possibility of replacing the boarding step entirely came to light and that's when the brainstorming shifted towards having a more

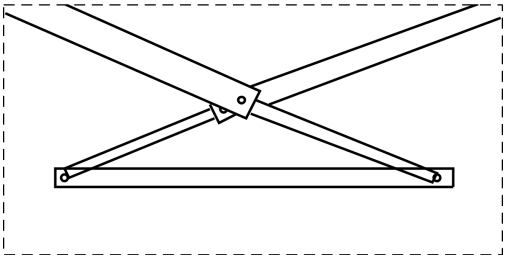

(a) Brainstorm Idea Car Lift

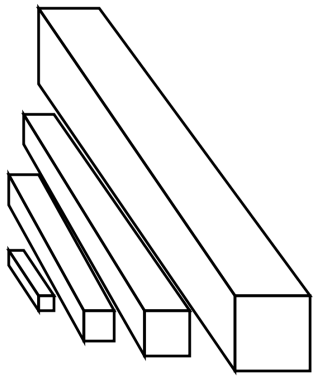

(b) Brainstorm Unfolding Stairs

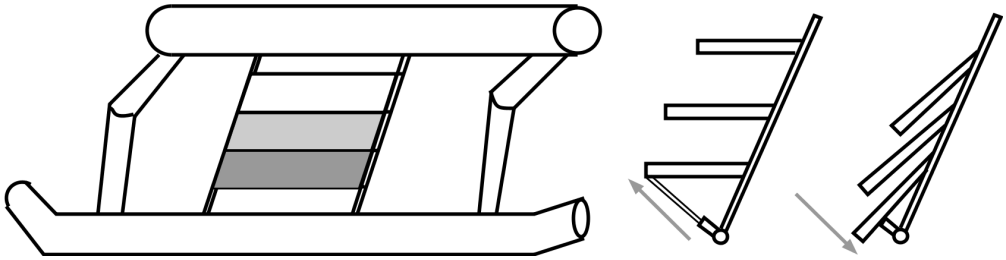

(c) Brainstorm Pneumatically Actuated Stairs

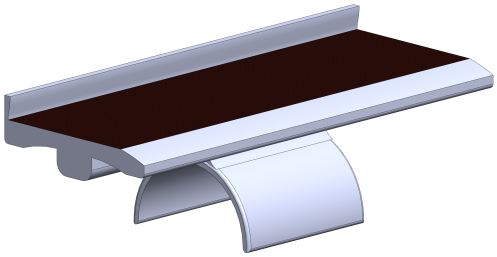

(d) First design idea

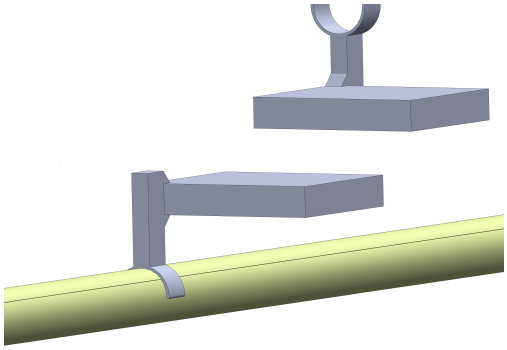

(e) Second design idea

Figure 3.1: Initial Sketched Ideas

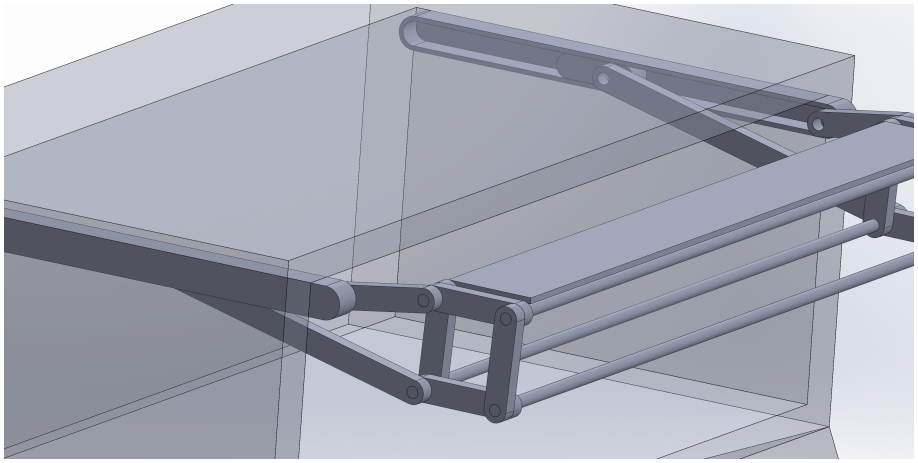

Figure 3.2: Foldable stair in box.
Adapted from Rajashekhar et al.

complex version that could be more ergonomic and resemble actual stairs. The Unfolding Stairs Mechanism (Figure 3.1b) was modelled as seen in Figure 3.2 and its mechanism was partially developed according to the paper by Rajashekhar et al.[20] in which the stairs are actuated linearly via a Rail-Slider Mechanism.

This idea was dismissed because the equipment would end up having a considerable size, hence colliding with existing equipment in the aircraft.

3.2 Final Design Modelling and Improvement

The final concept design (Figure 3.3) emerged from a brainstorm in a meeting with AHD in which details were discussed and both the simple step and box concepts were dismissed in lieu of fully replacing the Board Step.

This idea called for an additional retractable step, the subsequent step was to figure out which mechanism to use and how to employ it to ensure its viability. The first sketches for the mechanism can be seen in Figure 3.4. These were initially based solely upon the sketch sent over from AHD but the last one in Figure 3.4 already resembles the final version a great deal seeing as how it was the basis for it.

The final design version of the Add Step mechanism is a take on the 4-bar linkage in which one of the bars (the Board Step) is stationary. This allows translational and rotational movement which enable the Add Step to be hidden from sight when not in use and be extended out towards the user when necessary.

Initially, it was meant to be mounted as shown in Figure 3.5 and its top bolted to the bottom of the Board Step. This would result in a very block-like design which could compromise the deployment and usage of the floats (Figure 2.2).

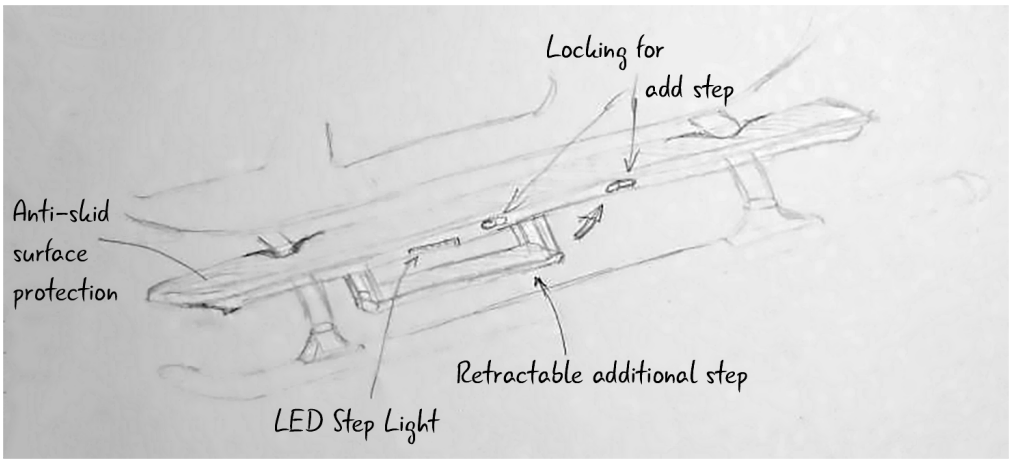

Figure 3.3: Design sketched during brainstorming session

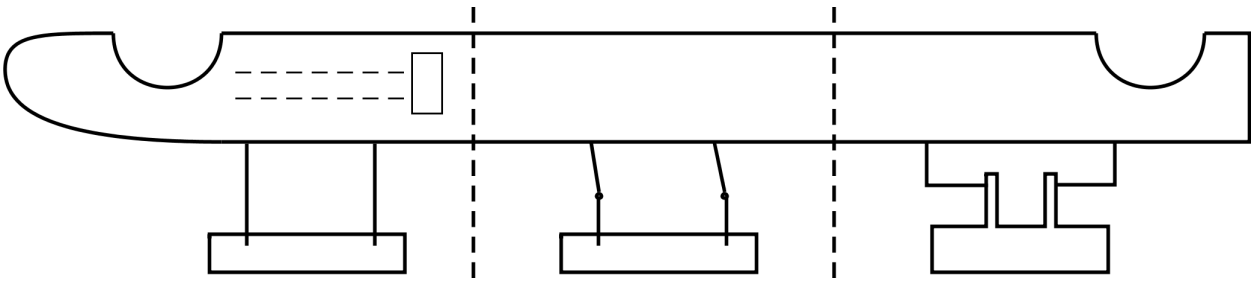

Figure 3.4: First sketched ideas for the extension and retraction mechanism in the Additional Step

As stated in Section 2.3, a 200 mm rise is still comfortable and so the goal was to achieve that rise between the floor and the Add Step as well as between the Add Step and the Board Step, leaving a 400 mm rise to the helicopter itself. This last step is expected to be the highest but not the worst ergonomically since the user can hold on to the door handles as well as the inside walls to aid climbing, something that is not possible with the first two steps.

The goal now was to make it so the Add Step mechanism would fit under and behind the Board Step which is a requirement issued to prevent interference with other equipments. This was achieved by iteratively reworking the Add Step sub-assembly and changing overall geometry of parts (thickness, angles between faces, pin-holes locations) as well as the fit and length of the link parts with an additional goal in mind to achieve the ideal rise of 200 mm (half the rise from the floor to the Board Step) all the while maintaining a small enough size to fulfil the initial objective.

Altering the length and curvature of the link parts is an iterative heavy process which took weeks until the optimal ratio was found. There were several dimensions being considered throughout these iterations and these are visible in Figure 3.5 and listed below:

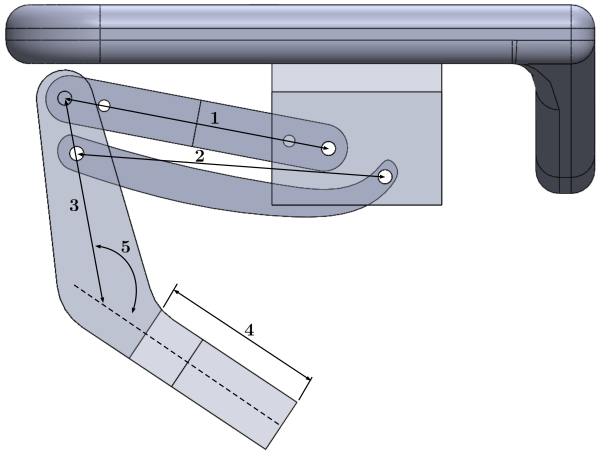

Figure 3.5: Dimensions for Additional Step Mechanism iterations

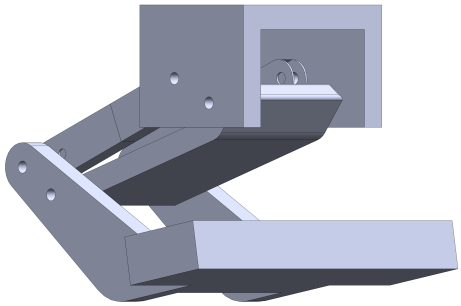

Figure 3.6: Additional Step Mechanism mid-way through iterations

1. Leg Link Length;
2. Arm Link Length;
3. Additional Step Connector Length;
4. Additional Step Depth;
5. Angle between Step and Step Connector.

Aside from the enumerated items previously mentioned, the overall shape and dimensions of all parts had to be taken into account. Figure 3.5 illustrates the difficulty of fitting this mechanism behind and below the Board Step. Figures 3.5 to 3.8 illustrate part of the process to improve the utility of the Add Step and the incremental improvements such as the one in Figure 3.7 added up to the final model.

When the ergonomic dimensions were at the desired values there was still a need to lock the Add Step in its in-use position as well as figure out a way to secure it while not in-use. The lock for in-use can be seen in Figure 3.9a as being a contact between the links while a

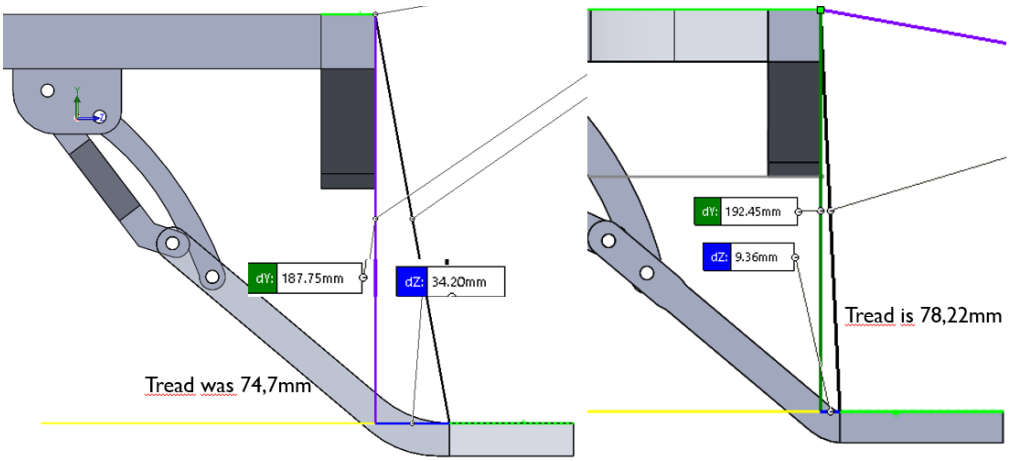

Figure 3.7: Ergonomic dimensions improvement on the Additional Step

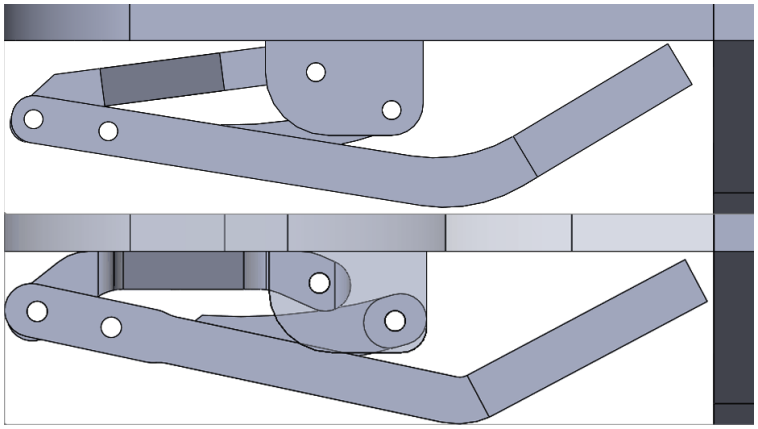

Figure 3.8: Final iterative improvements on the Additional Step

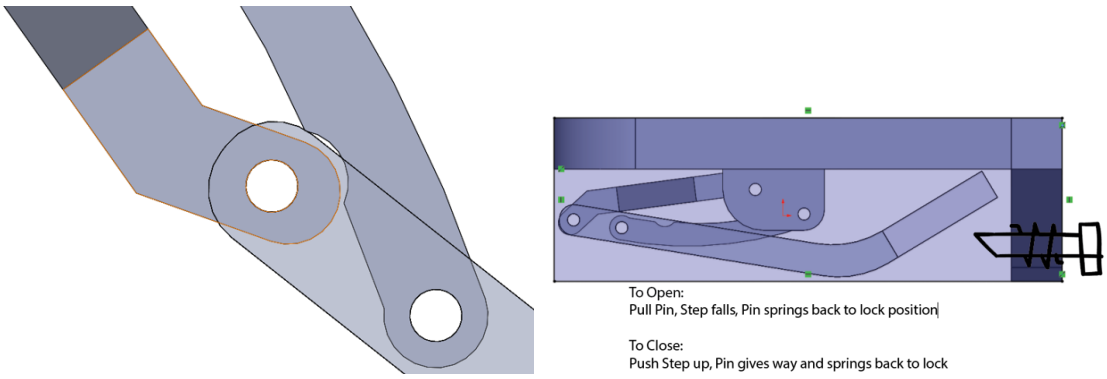

(a) In-Use locking of the Additional Step by the link parts

(b) Lock Pin Sketched concept

Figure 3.9: Locking mechanisms for in-use and flight

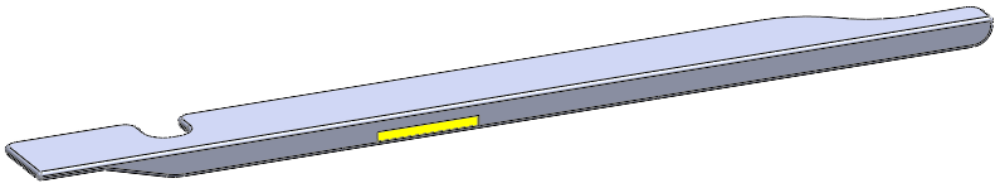

Figure 3.10: Boarding Step sub-assembly

lock pin (Figure 3.9b) secures it in place when not in-use. This lock pin was simply sketched as a concept and left aside as it wasn't relevant at the time but is surely an important part of the concept which should be pursued in the future.

After all the improvements and design changes were made to both the Board Step and the Add Step as well as its link parts, the whole creation aspect was close to finished. The next step was to figure out which fixtures to use so that the Board Step would actually connect to the helicopter, therefore becoming a full concept. It's worthy of note that the Board Step was at this point in time split into two parts as can be seen in Figure 3.10. This was a measure taken to prevent having to mill it from a full block of aluminium and wasting material.

The fixtures that AHD uses currently are already a perfect fit for the helicopter, so they were re-used with the assistance of a new C-shaped part to help level Board Step as seen in Figure 3.11. The design was now completed and ready to be simulated with FEM. Chapter 4 will include some changes made to the design to accommodate the needs established by the loads during simulation. The starting model to reach the simulation phase is displayed in Figure 3.12 and is comprised of nine (9) parts, two (2) of which are the C-shaped part (Figure 3.11) leaving a total of eight (8) unique parts, six (6) of which designed by the student.

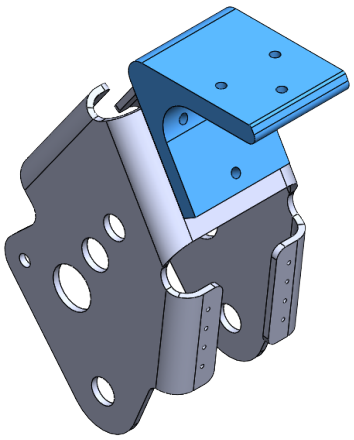

Figure 3.11: One of the fixture assemblies including the C-shaped part highlighted in blue

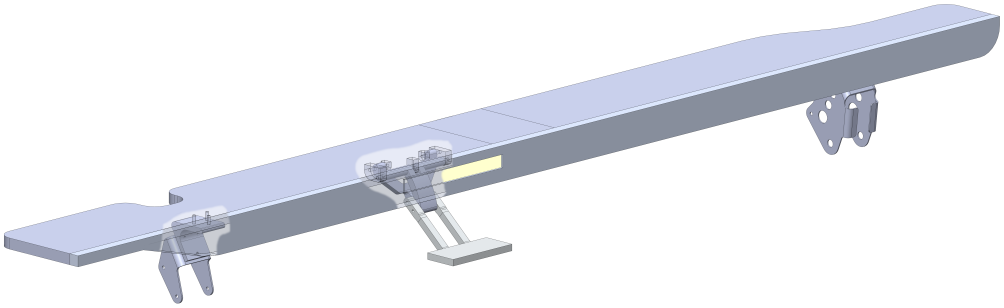

Figure 3.12: Finished Board Step design with Add Step Assembly and Fixtures

Chapter 4

Analysis and Simulation

The current chapter covers all the analysis and simulations that took place after the initial design of the Board Step, Add Step and all component parts. The design of the parts is modified throughout the current chapter according to the obtained results.

4.1 Solidworks Simulation Studies carried out

This section will briefly introduce some of the FEA capabilities that SW has, namely the ones used in this project.

4.1.1 Static Simulation

All Static Simulations in SW function around the same input-output system. The input parameters are:

- Model or models that take part in the simulation;
- Joint groups for parts with beam elements;
- Shell manager for parts with shell elements;
- Model or models' material and material properties (usually assigned from within SWs' very own material library but can be edited);
- Connections;
- Fixtures;
- External Loads;

- Meshing.

The connections category can simulate bolts, pins, rivets, springs, all types of flexible supports, bearings and bonding agents such as adhesives or welds. It's also where component contact is defined and in decreasing complexity it can be with no penetration, bonded or allowing penetration. The fixtures category allows the user to restrain certain assets within the model, be they vertices, edges, faces or whole bodies in all DoF. The external loads category contains forces, torque, pressure, gravity, temperature induced forces and several others.

Meshing is very important in simulation. Not only will it directly affect the computation power - and therefore time - needed for it to be ran but also influence the results. SW has a very in-depth meshing system that allows for it to be defined as finer or coarser in each individual face on a model. A good starting point is to assign a generic mesh density to the model, which is chosen by the software usually in order to have at least two (2) elements in the thinnest thickness of the model. The correct approach is to then apply mesh control to areas that are known to be likely stress hot-spots - holes, thickness changes or low-radius fillets are some examples.

The outputs of Static Simulations are Stress graphs (default is von-Mises criterion), Displacement graphs (default is resultant), Equivalent Strain graphs, Result Forces and even Stress HotSpot Diagnostics. This last one is a tool that reads off of the existent Stress graphs, diagnoses hot-spots and marks the elements that fit that description allowing the user to more easily determine which areas of a model need tinkering.

4.1.2 Parametric Optimization

Known as a Design Study within SW, a parametric optimization will vary certain design parameters of a part within a given range and optimize it towards a set goal all the while respecting however many constraints the user decides to add. In the case that constraints or the goal include any of the outputs of a Static Simulation (values of stress, displacement or frequencies), SW requires a Static Simulation to be ran beforehand to serve as a guideline.

The software will then select, out of all scenarios, the optimal one and show the values of the chosen parameters as well as the constraints and goal.

4.2 Additional Step

4.2.1 Model Description

Depending on the simulation that's ran and what answers are sought out, the Add Step

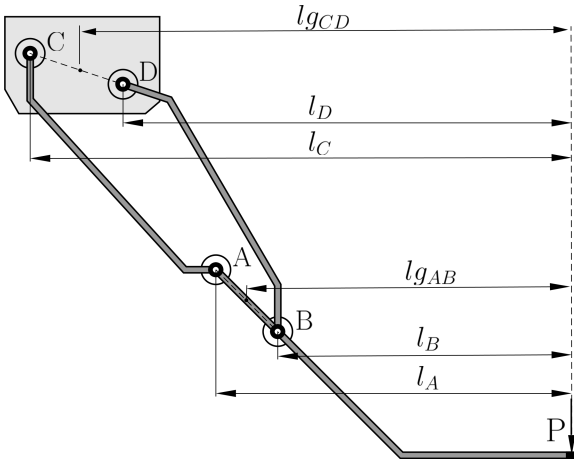

Figure 4.1: Additional Step's Assembly Free Body Diagram

model is simulated in different ways. As an example, the simplest version was used to validate the shear force applied to the pins connecting it to the arm and leg links (refer to Section 4.2.5). By increasing the complexity of the simulation it's then possible to obtain results that better represent reality.

The Add Step model assembly includes the Add Step itself as well as the arm and leg links and all eight (8) pins. Its nomenclature is visible in Figure 4.1 as a 2D representation. The material used for the simulations was referred by AHD and is an Aerospace-grade Aluminium alloy heat-treated and artificially aged. The most meaningful properties for this particular use-case are its Young Modulus of 72 GPa and Yield Strength of 505 GPa. By using the same material throughout the assembly galvanic corrosion can be avoided.

4.2.2 Simulation Setups

The Add Step went through four (4) phases during its simulation: Static Simulation, Parametric Optimization, Design Change and Static Simulation again - visible in Figure 4.2.

The Static Simulations don't have any connection parameters, seeing as how those are only applicable to assemblies. The fixture of the Add Step is a Fixed-Hinge (Figure 4.3) which only allows for rotation around the axis of the pin-holes. The external load is a force whose value is provided in AHD's Requirements Specification [4] and is applied on the edge furthest away from the pin-holes. The mesh was assigned generically as mentioned in Section 4.1.1 and then refined near the pin-holes and again near the thickness change, to better evaluate the stress in those more critical locations (Figure 4.4).

4.2.3 Simulations Results and Discussion

The first simulation of the Add Step (Figure 4.2a) was compared to a version with

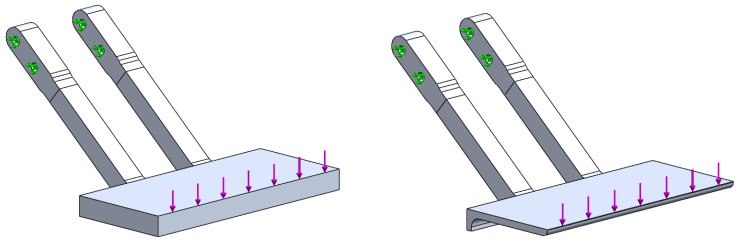

(a) Initial Simulation

(b) Optimized Additional Step

Figure 4.2: Evolution of the Simulation process of the Additional Step

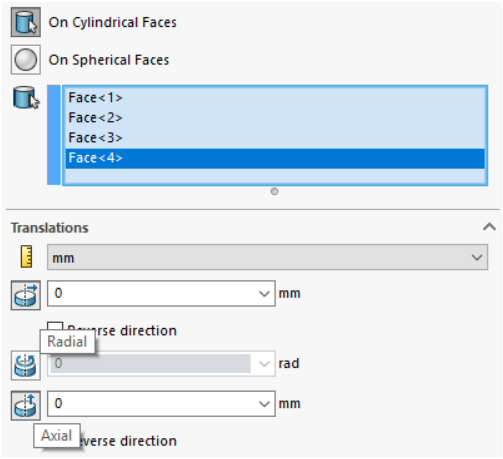

Figure 4.3: Fixed-Hinge Fixture in SolidWorks

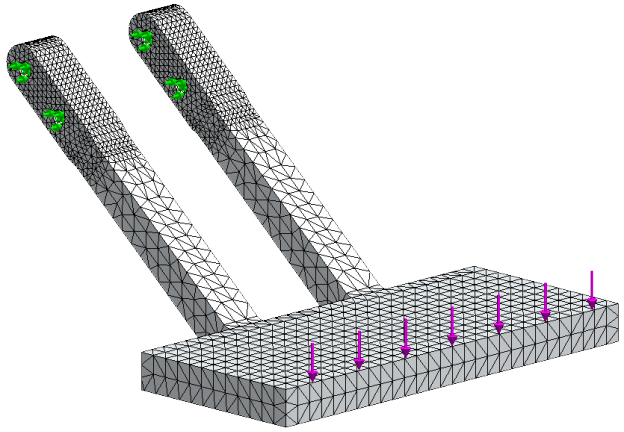

Figure 4.4: Meshing of the Additional Step's first Static Simulation

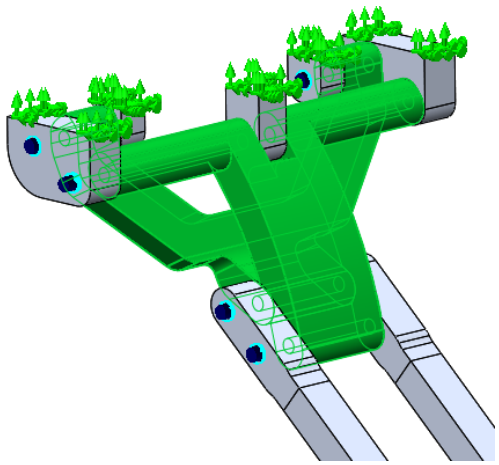

Figure 4.5: Assembly's Static Simulation view with Bonded-Arms detail in green

connections to the arm and leg links via pins in which these were bonded as is visible in Figure 4.5. The way to compare these simulations was to retrieve the result values for the pins from the Bonded-Arms simulation and result values for the fixtures from the Fixed-Hinge simulation. These values were meant to be the same and their relative errors were calculated using Equation (4.1) where *Bonded* and *Fixed* are the result values for the Bonded-Arms' pins and Fixed-Hinge's fixtures respectively.

$$\epsilon = \frac{Bonded - Fixed}{Bonded} \cdot 100\ \% \tag{4.1}$$

After making sure that the simulations were comparable, the results of the pin shear values were compared to the hand calculations made in Section 4.2.5. This was an extra step taken in order to validate the results and to be certain the assemblies were properly put together. It was then time to simulate the Add Step on its own using the Fixed-Hinge models shown in Figure 4.2.

The simulation from Figure 4.2a yielded very satisfactory results, with a maximum stress $\sigma_{max} = 192$ MPa, yielding a FoS of 2.6 in its most critical element, visible in Figure 4.6. This meant the part was oversized and could be tweaked, that's where the Parametric Optimization comes in.

As mentioned in Section 4.1.2, a Parametric Optimization makes use of set of design parameters - three (3) in this case - and varies them within a given range. Observing Figure 4.7, one can define the variables as follows: the Bottom Reinforcement, which maintains some of the rigidity from the original part; the Front Fillet and Step Thickness, which will vary to allow the mass to reduce, all the while maintaining enough material for the Add Step's front end not to displace too much (Figure 4.7).

The simulation went through 70-odd iterations and obtained an optimal solution which compromises slightly on stress in order to reduce the weight up to 47 % (Figure 4.2b). This

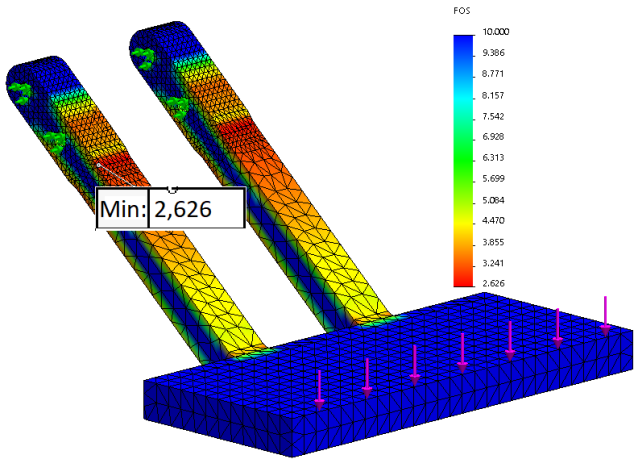

Figure 4.6: Factor of Safety distribution on the Figure 4.2a Model

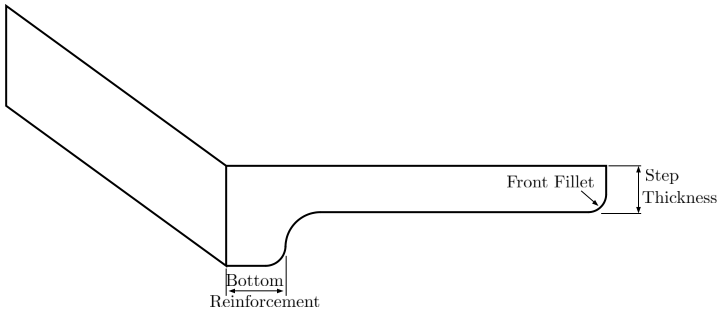

Figure 4.7: Additional Step's Parametric Optimization's parameters diagram

design went through the same Static Simulation as the one from Figure 4.2a in order to confirm the results from the Parametric Optimization with a more refined mesh and the maximum stress σ_{max} went up to 218 MPa which is still well within the acceptable range for this material.

Some of the issues that arose after this simulation were that by applying force to either side of the model the pin-holes would suffer enough torsion to make the tension spike upwards of 400 MPa rendering the part useless. Another issue was the current size of the Add Step: at 180 mm in width and a tread of under 80 mm, it was just not big enough to be a viable step.

4.2.3.1 Remodelling and Final Design Simulation

In order to obviate the size issues previously mentioned some changes had to be made to the original design. The width could be doubled without interference, but the other dimensions were more challenging. While remodelling the Add Step, the leg and arm connection links also needed to be tuned and so the biggest hurdle to overcome was to fit all of the components below and behind the Board Step once again. To help with this, SW has a

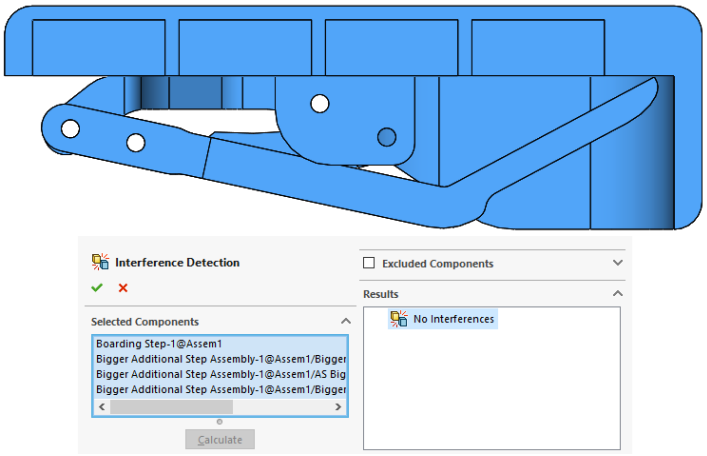

Figure 4.8: Interference Detection Tool in SolidWorks

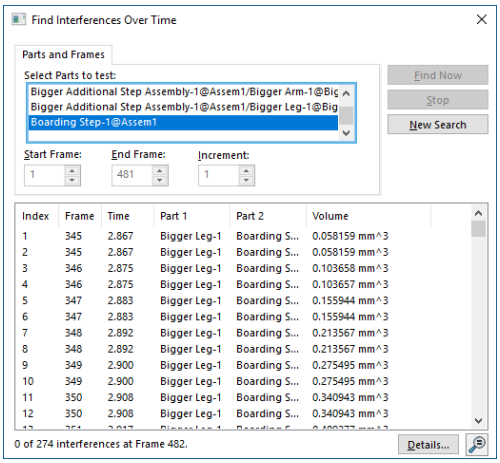

Figure 4.9: Find Interferences Over Time from Motion Analysis in Solidworks

tool named *Interference Detection* which helps in finding if the parts are intercepting other neighbouring components. Its use is visible in Figure 4.8, however, the only thing this tool doesn't do is detect interference in a several positions at once. This is something the motion module can help with, seeing as how it has a tool named *Find Interferences Over Time* which is a perfect fit for the issue being tackled at the time. Although Figure 4.8 shows that there is no interference while the assembly is not in use, Figures 4.9 and 4.10 reveal the frames in which interference occurs between the selected parts as well as the start and end frames for the motion analysis in which interference detection was ran. After fitting the assembly and having made the necessary adjustments to solve its geometric challenges it was time to solve the structural flaws that still existed within the model. The modelling and simulation changes made to the arm and leg links are detailed in Section 4.2.4.

In order to combat the tension spikes some solutions were proposed:

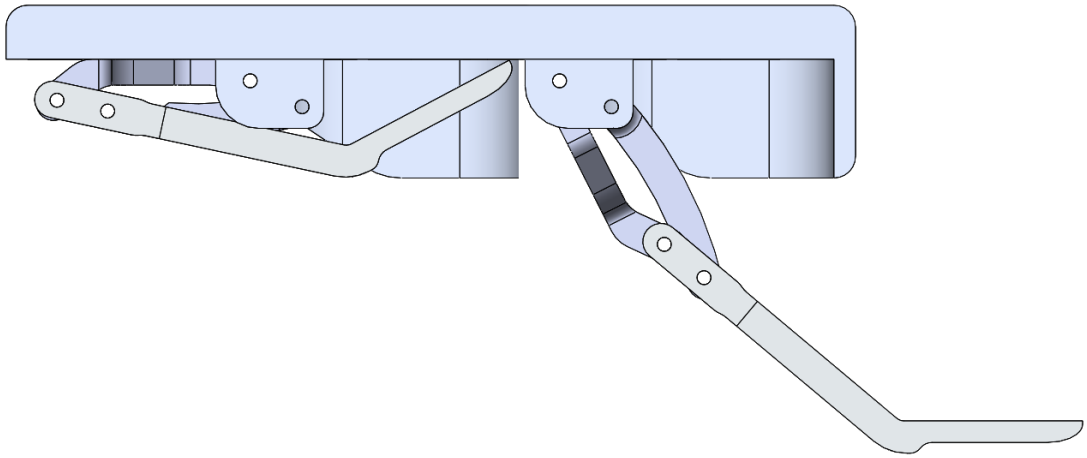

Figure 4.10: Starting and Ending frames for the Motion Analysis

- Increase thickness of the Add Step's bars;
- Increase the number of bars;
- Shift the bars' locations.

Doubling the thickness of each bar would result in the same tension spike as the whole step was already twice as big and such a large thickness would result in an overly block-like design. Increasing the number of bars may sound like a viable option at first but since the depth of the Add Step cannot be changed due to the Board Step's size constrictions, the extra bars would block the users feet from being able to properly stand on it. So the last option was to relocate the bars to the edges allowing for a gap in the middle wide enough for a size EUR 45 boot to fit comfortably. The bars' thickness was increased to accommodate the overall scaled design and all the edges were smoothed and sharp corners avoided to decrease the risk of there being any geometry singularities that could jeopardize the static simulations. The final design of the Add Step is visible in Figure 4.11 and although it may still be subject to minor changes, its overall shape and size fulfils the goals set upon in the start of this chapter.

It was then time to perform Static Analysis on the final design of the Add Step. The meshing procedure followed the same guidelines mentioned in Section 4.1.1, by increasing the number of mesh elements in known problematic areas such as the thickness change and around the holes as well as beneath the step, by the bottom reinforcement (visible in Figure 4.12).

The force was applied at the edge furthest away from the holes (as mentioned in Section 4.2.2) and the holes had their radial and axial movement restrained (Fixed-Hinge). The simulation yielded the best Stress results obtained so far (Figure 4.13a) while maintaining a maximum displacement under 3 mm (Figure 4.13b).

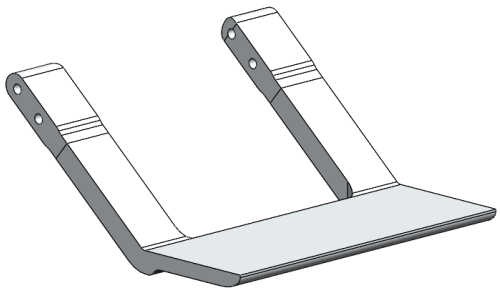

Figure 4.11: Final Additional Step Design

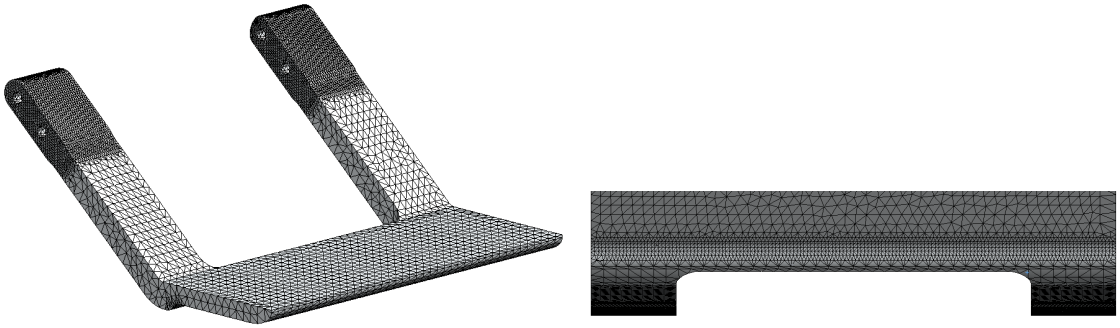

(a) Main view of meshed model (b) Detail of Mesh viewed from beneath

Figure 4.12: Meshing of the Additional Step's Final Design

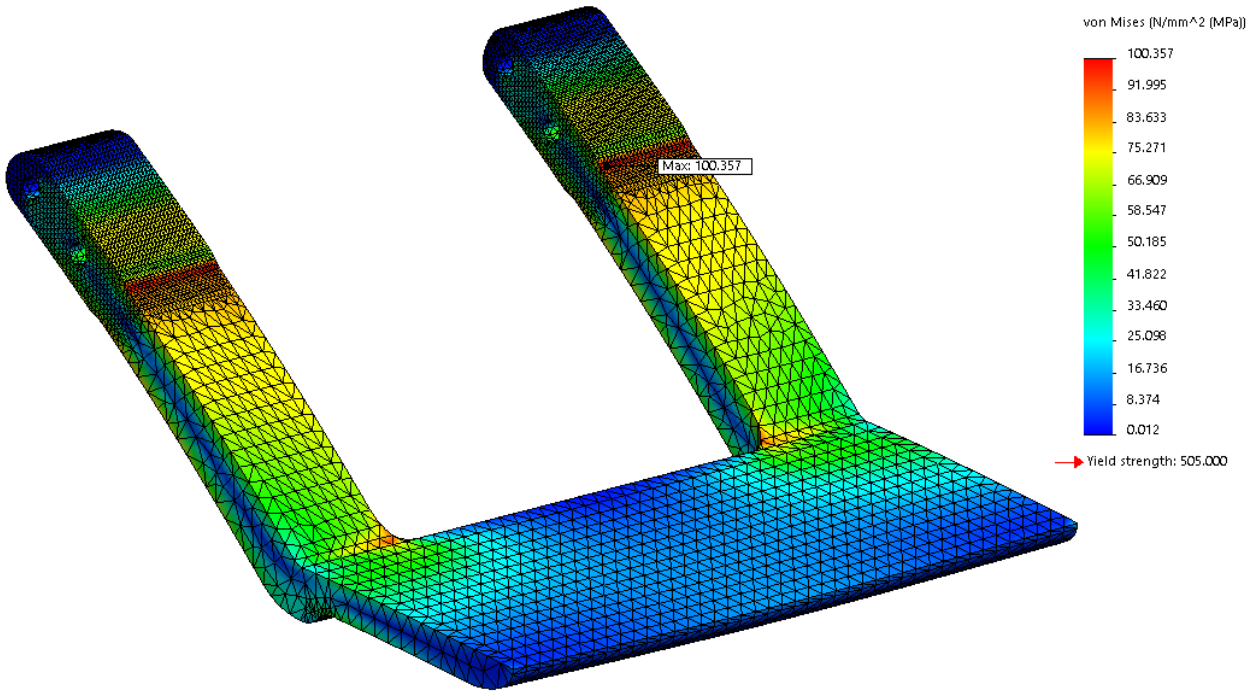

(a) Von-Mises Stress graph of final model

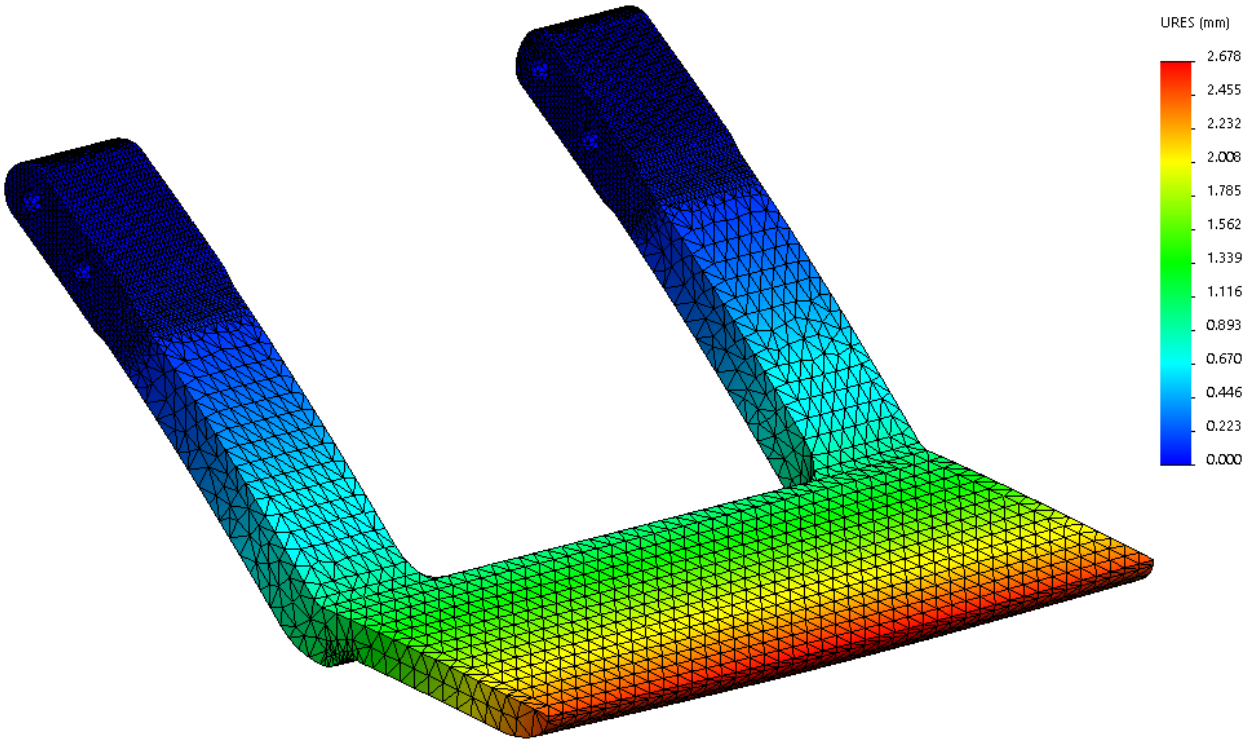

(b) Resultant Displacement graph of final model

Figure 4.13: Static Analysis Simulation Outputs

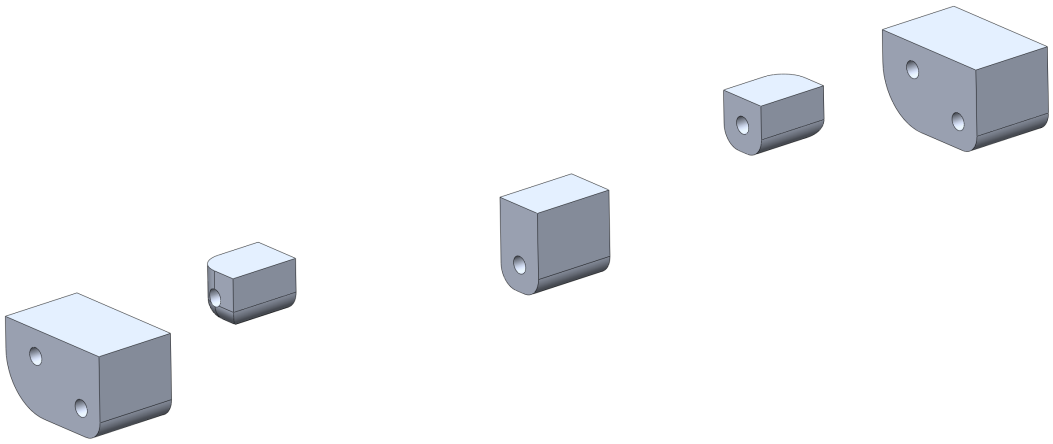

Figure 4.14: Biscuits located underneath the Boarding Step (Boarding Step not visible)

4.2.4 Arm and Leg Links

The Arm and Leg links' analysis followed the Add Step's closely. They were in fact done simultaneously as the assembly's functionality is structured around all three (3) parts as shown in Figure 4.5. Also visible in said Figure is the simplification taken into account while simulating, which is the bonding of both links. This allows SW to treat the two contacting links as a single part, alleviating the processing power needed to simulate no-penetration contact between them.

Seeing as how to properly simulate the links there is inherently more complexity associated with the analysis, it will be thoroughly explained. To more easily structure this explanation, it will follow the enumeration below:

1. Model and Parts;
2. Interactions;
3. Meshing, External Loads and Fixtures;
4. Results.

4.2.4.1 Model and Parts

As mentioned previously the assembly's functionality revolves around the links and the Add Step and their relative movement, but this is only possible if there's a fourth link allowing the whole to behave such as a four-bar linkage would. This last link is comprised of a very specific piece of another part which are biscuits located in the underside of the Board Step (Figure 4.14).

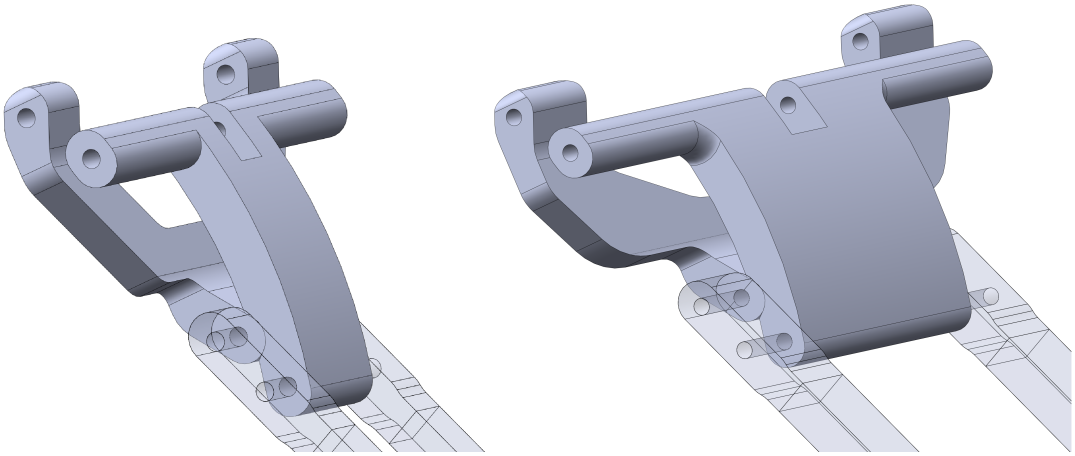

Figure 4.15: Differences previous to and after scaling of the Links

These biscuits came to be during the design process between the steps shown in Figure 3.6 and Figure 3.8 as an attempt to save enough height space to fit the whole Add Step assembly behind the front of the Board Step. In truth, the whole Board Step is the fourth link since these biscuits are a piece of it, but in order to save time during the analysis and prevent software crashes, they were cut-off from the Board Step and assembled as an individual part, as is visible in Figure 4.5.

Section 4.2.3.1 describes in full the steps taken when scaling up the Add Step model and the process was very similarly applied to both links. Figure 4.15 illustrates the differences before and after scaling.

4.2.4.2 Interactions

Visible in Figure 4.5 are the pins, in blue, that allow for interaction between the biscuits, links and Add Step. These are locked in place to prevent axial movement by the cyan retaining rings. Since SW only allows for a single shear force application per connector, there needs to be a pin per shear area rendering a total of twelve (12) distributed as such: four (4) on pin-holes **C**, four (4) on pin-holes **D**, two (2) on pin-holes **A** and two (2) on pin-holes **B** (Figure 4.16). Each of these simulated pins will restrain only axial and radial movement, allowing for rotational movement, performing a Moving-Hinge similar to the Fixed-Hinge mentioned in Section 4.2.2

The contact between parts was also set at this stage and to best simulate the real conditions it was set to no-penetration contact which is the most demanding in terms of computing power but is also the only one among the three (3) mentioned in Section 4.1.1 that accurately simulates the reality of the system.

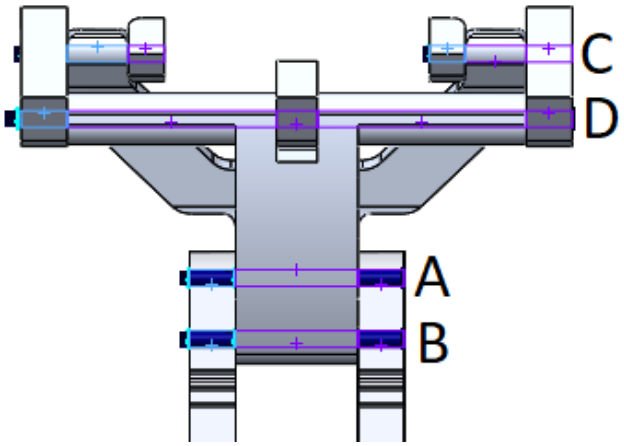

Figure 4.16: Illustration of Connection Pins in Additional Step Mechanism Assembly

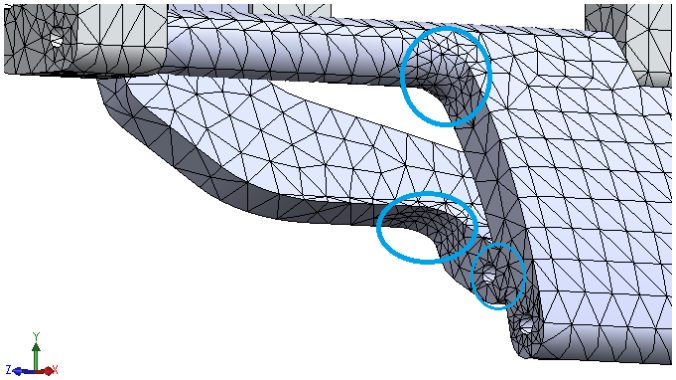

Figure 4.17: Meshing of the Arm and Leg Links with blue highlights in expected problematic areas

4.2.4.3 Meshing, External Loads and Fixtures

Meshing followed the guidelines mentioned in Section 4.1.1, increasing the number of mesh elements in known problematic areas such as in bends on the Arm and Leg Links as well as in the areas mentioned at the end of Section 4.2.3.1. Some of the expected problematic areas are highlighted in Figure 4.17.

This analysis also included gravity and the force described in Section 4.2.2. Only the biscuits were fixed in all DoF at their flat side which would be part of the Board Step. The simulation was now ready to be ran.

4.2.4.4 Results

The highest stress was recorded in the fillet area as indicated in Figure 4.18 with an approximate value of 436 MPa. This is quite a high value, rendering a FoS of only ≈ 1.18.

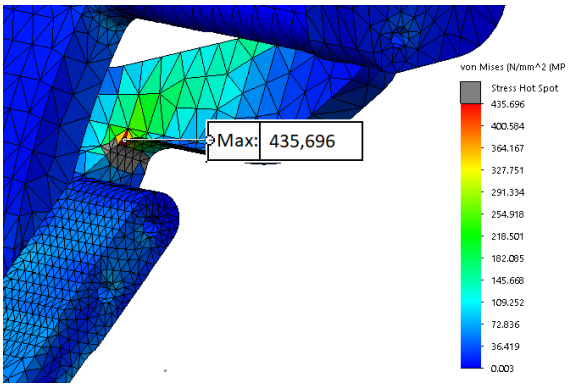

Figure 4.18: Von-Mises Stress graph of links assembly

It's worthy to note that this happens due to the scaling the Add Step was subjected to, as the part wasn't scaled by the same value in all directions.

The displacement value for the edge of the Add Step was recorded at 16 mm which is acceptable.

Since these parts will be subjected to several loads throughout their life it would be extremely relevant to perform a fatigue study on them with the in-use load case of 1 person on the Add Step in an assembly. This was not done in this project but is mentioned as something to do in the future (refer to Section 6.6).

4.2.5 Pins

In order to calculate the diameter required for the pins to handle the shear force there are some assumptions to be made:

- All parts are perfectly rigid;
- The Arm and Leg links' surface contact is bonded, as are the ones between the links and the Add Step;
- All of the force is applied on the edge that is furthest away from the pin-holes;
- Gravity is excluded from all calculations.

Let P be the force applied to the edge (visible in Figure 4.19) and so the Total Shear Force applied for **A** is given by Equation (4.4). The equation is the same for all four (4) pin-holes with differing distances and geometric centres.

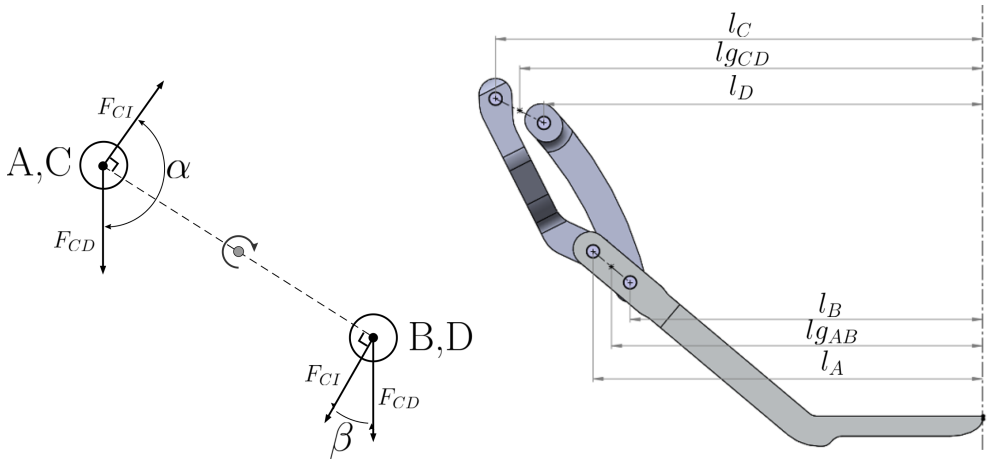

Figure 4.19: Pin-holes Free Body Diagram and Add Step side view

$$F_{CD} = \frac{P}{N_{SP}} \tag{4.2}$$

$$F_{CI} = \frac{P \cdot lg_{AB} \cdot \frac{1}{2} l_{AB}}{N_{SP} \cdot \frac{1}{2} l_{AB}^2} \tag{4.3}$$

$$F_{CT} = \sqrt{F_{CD}^2 + F_{CI}^2 + 2 \cdot F_{CD} \cdot F_{CI} \cdot \cos(\theta)} \tag{4.4}$$

Seeing as how the F_{CD} and F_{CI} are the same in both pin-holes, the determining factor in the magnitude of F_{CT} will be the angles (α, β). Whichever is closest to 0 will result in a higher magnitude which will be used to determine the minimum diameter of the pins to be inserted. In both scenarios (**AB** & **CD**), β yields a higher magnitude of F_{CT} (note that $\beta_{AB} \neq \beta_{CD}$).

$$A_p = \frac{\pi \cdot \phi_{ph}^2}{4} \tag{4.5}$$

$$\tau_{op} = \frac{F_{CT}}{A_p} \tag{4.6}$$

$$\tau_{ADM} \approx \frac{\sigma_{ys}}{2} \tag{4.7}$$

Equation (4.8) borrows from Equations (4.5) and (4.6) and the approximation described in Equation (4.7) to write a relation between σ_{ys} and the diameter of the pin-holes. This allowed to choose a diameter based on the material that's already being used for the Landing Gear in AHDs' helicopters.

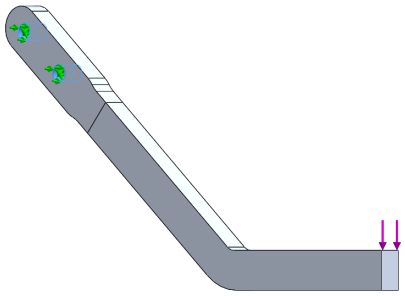

Figure 4.20: Simplified Additional Step model used to compare shear force values with analytical results

$$\begin{aligned} \tau_{op} \leq \tau_{ADM} \Leftrightarrow & \frac{F_{CT} \cdot 4}{\pi \cdot \phi_{ph}^2} \leq \frac{\sigma_{ys}}{2} \Leftrightarrow \\ \Leftrightarrow & \sigma_{ys} \geq \frac{4 \cdot F_{CT}}{\pi \cdot \phi_{ph}^2} \end{aligned} \tag{4.8}$$

Of course these results weren't final since they were based on the assumptions that were previously mentioned. They were however a step towards validating results on the CAD models. This was first achieved by simulating the Add Step alone with the Fixed-Hinge fixture (Figure 4.3) which only allows for frictionless rotation on pin-holes A and B around their axis. The simplified model used for this step is visible in Figure 4.20.

Using the Result Force tool on SW allowed for comparison with the values obtained from Equation (4.4). The average relative error between the values was of 0.17 % and was calculated the same way as in Section 4.2.3's Equation (4.1) yielding Equation (4.9).

$$\epsilon = \frac{HC - SW}{SW} \cdot 100 = 0.17\ \% \tag{4.9}$$

These values were then used as a basis for the more complex model assembled as shown in Figure 4.1. The model was connected to the biscuits on the underside of the Board Step which were fixed in all six (6) DoF and the parts were connected to each other via pins as shown in Figures 4.16 and 4.21.

If the values for F_{CT} for pins **A** and **B** are the same between simulations, then the simulations are valid and their results correct. It is then appropriate to assume the values for **C** and **D** are also valid. The simulation was then re-run with the effect of Gravity as well as No Penetration Component Contact. The highest Shear Force value for pins was then used as an input for Equation (4.8) and the diameter was obtained. Afterwards, all the parts were changed to accommodate the new higher diameter and were simulated again to confirm the change didn't compromise the remainder of the assembly.

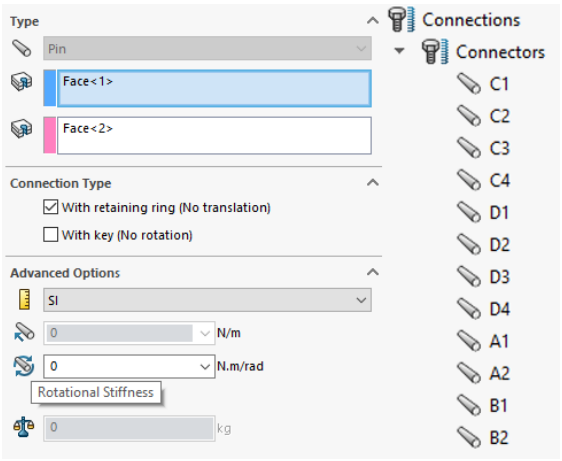

Figure 4.21: Connection Pins from the Additional Step Mechanism Assembly as applied in SolidWorks

4.3 Boarding Step

4.3.1 Model Description

At its core the Board Step is considered a shell and was simulated as such in its second iteration. But first, as is visible in Figure 4.22, some simpler versions were tested. The beam was compared with analytical calculations that followed the Universal Equations (Section 2.2.1.1), while the shell version was compared to the calculations made according with the Rayleigh-Ritz Method (Section 2.2.1.2).

The Board Step went through several design changes throughout this analysis and simulation stage and those changes were, for the most part, justified by the results of simulations. Some were however purely cosmetic or to facilitate the manufacturing process or even to allow a change in materials to a composite or even composite-aluminium hybrid from the original aluminium alloy.

The previously mentioned Figure 3.12 illustrates the Board Step as it was upon reaching the simulation stage of this work. The design varied a lot to accommodate the evolution of all the parts as well as the fixtures. One of the main differences was the addition of a side-plate in order to increase the rigidity of the Board Step which was initially meant to be bolted together.

As was the case in Section 4.2 the Board Step also went through some weight-rigidity optimization in which material was removed from the bottom part in the way of rectangular parallelepipeds. This allowed the ribs and struts that weren't removed, to maintain a lot of the rigidity while considerably reducing the weight. This model alongside the shell of the original and the original were aptly named Default, Removed Material and Complex Shell.

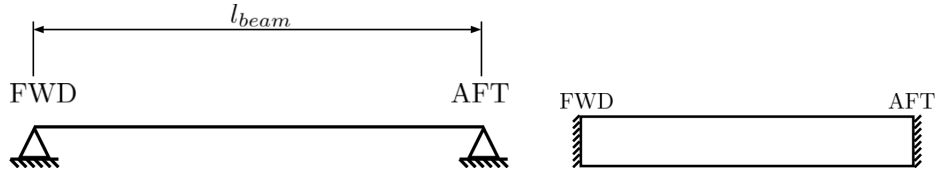

(a) Boarding Step as a Beam (b) Boarding Step as a Shell

Figure 4.22: Simplified versions of Boarding Step

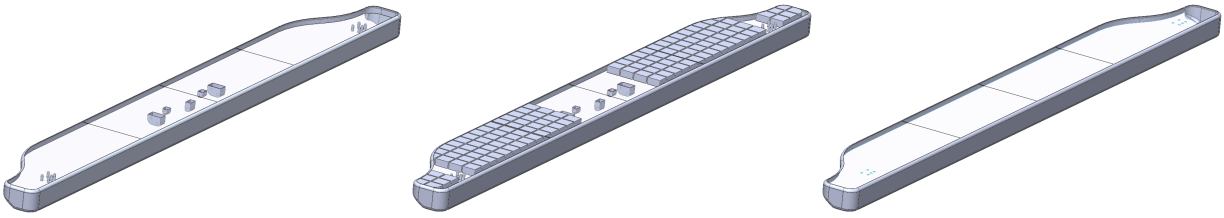

(a) Default (b) Removed Material (c) Complex Shell

Figure 4.23: Three models of the Boarding Step. Some surfaces are transparent for easier perception of the underside of the model

A isometric view of each of these models is visible in Figure 4.23.

The material used for the simulations was also referred by AHD and was expected to be the same Aerospace-grade Aluminium alloy mentioned in Section 4.2.1. The Complex Shell's model was simulated in a composite sandwich and its definition is described in Section 4.3.4.

4.3.2 Early Simulation

The Board Step was first studied as a Beam and, as is visible in Figure 4.22a, the fixture was thought to be simply supported - restricting movement in all 3 axis but allowing free rotation about them. This was however previous to the models being made available by AHD and was later revised to being a fixed support.

The method used to calculate the maximum displacement for the beam model was the Universal Equations in which the beam was divided into four (4) elements. Each of these had a displacement approximation equation such as Equation (2.1).

These were then derived to achieve the equations for rotation, bending moment, shear and distributed load - Equation (4.10). The end result was achieved by solving the static equilibrium equations as well as the border conditions in order to obtain the resultant forces as well as the displacement mid-beam - where the external load was applied.

$$EIy \xrightarrow{\frac{\partial}{\partial z}} EI\theta \xrightarrow{\frac{\partial}{\partial z}} M \xrightarrow{\frac{\partial}{\partial z}} T \xrightarrow{\frac{\partial}{\partial z}} L \tag{4.10}$$

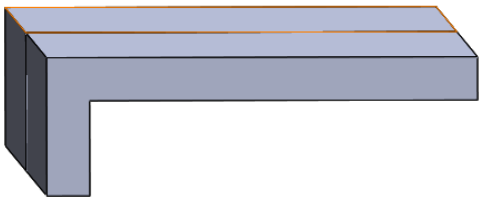

Figure 4.24: L Shaped Boarding Step Beam Simulation

Alongside the analytical calculations, a simulation was created and ran in order to compare values. In SW, the Structural Member tool was used to produce an L-shaped profile along the length of the Board Step (Figure 4.24). This profile already included the side-plate mentioned previously. By using the Structural Member tool instead of extruding the part normally, SW's simulation can recognize the parts as beam elements instead of solid bodies and mesh them as such (refer to Figure 2.7). The load was applied just the same as in the hand-written calculations: in three (3) equidistant points, the middle one being centred, according with AHD's Requirements Specification [4]. The mesh used in this simulation was somewhat coarse as its analytical counterpart only had four (4) elements.

The simple Shell model (Figure 4.22b) followed suit after validation of the Beam model. This model was solved analytically using the Rayleigh-Ritz Method (refer to Section 2.2.1.2). Since this method uses pressure loads instead of forces, the load was also distributed throughout the plate on the FEA. The mesh used in this simulation was again somewhat coarse as there's no reason to have it be fine. The simple shell model is visible in Figure 4.22b.

4.3.2.1 Solid Body Simulation and Redesign

Figure 3.10 illustrates the first model of the Boarding Step to be simulated as a solid body. Seeing as how it's a single model and not an assembly, there are no assembly connections to speak of. The fixtures on this particular model weren't finalized yet so it was simulated using Fixed Geometry on the faces illustrated in Figure 4.25. The goal with this was to mimic the Board Step being firmly fixed to the Landing Gear. The external loads included in this simulation were gravity and the weight of three (3) people. There was also a different load case in which the weight of a person was singled out into an area the size of a foot on the protrusion visible on the left-hand side of Figure 3.10. This load case was meant to mimic a pilot getting into the aircraft. The Board Step is also required to hold the floats loads mentioned in Section 4.3.3.

At roughly the same time as this occurred, a request was issued by AHD to make preliminary calculations for the Board Step if it were made out of a composite sandwich. It was concluded that the design had to undergo some changes and in order to re-design efficiently there were some key points to focus on:

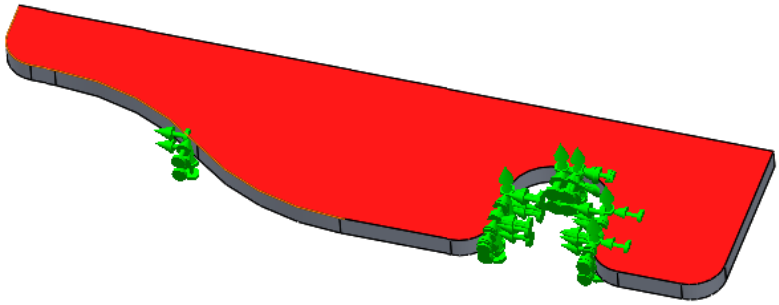

Figure 4.25: Fixed Geometry on the highlighted faces

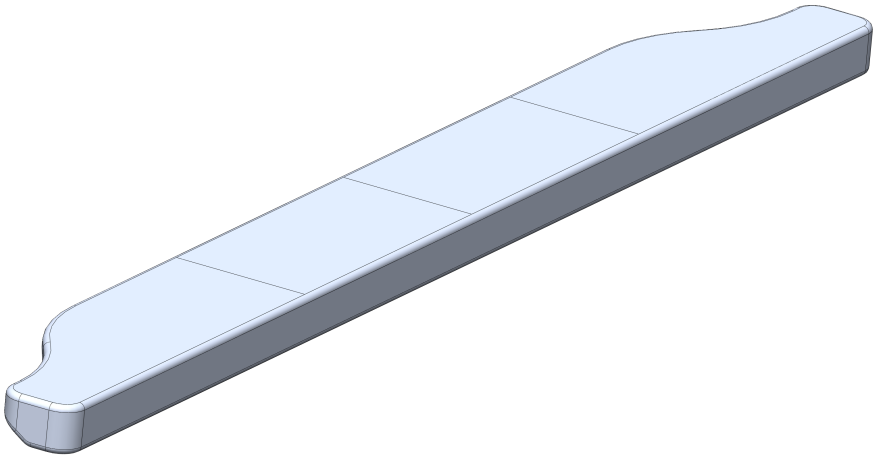

Figure 4.26: Boarding Step Model redesign

- In order to be made out of composite materials, it would be much easier and cheaper if the Board Step was a single part instead of two;
- The protrusion in flight direction was too long and would possibly compromise the connection with no added benefit;
- There was no reason for the asymmetric shape, so a symmetric alternative would decrease model complexity as well as ease manufacturing.

The protrusion in flight direction was first meant as a stepping area for pilots to enter the aircraft. However, after discussion with AHD it was possible to discern that pilots don't even use the current steps; most of the times they hold the door handle and jump into the aircraft. With this in mind, the new model was designed as is visible in Figure 4.26

Since the calculations for the composite materials version of the Board Step were mainly for weight reduction, an alternate option was also considered. It would be viable to remove material from underneath the Board Step leaving out ridges which would aid with rigidity all the while reducing weight significantly.

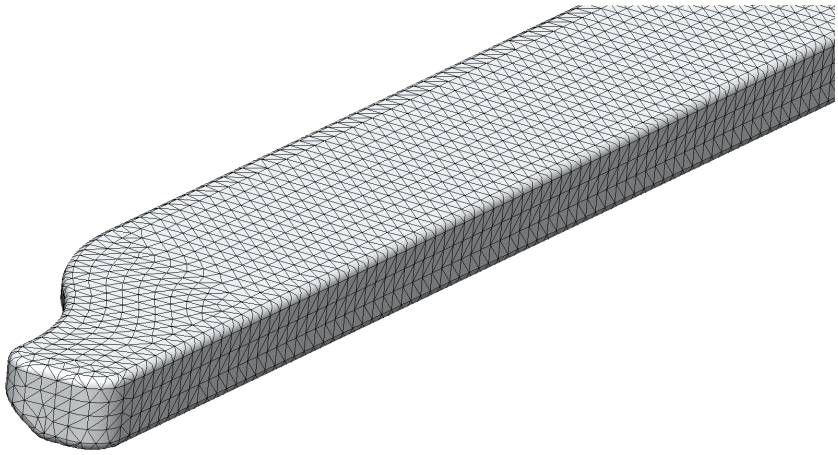

Figure 4.27: Meshing of Boarding Step's Default Model

4.3.3 Simulations Setups

There were several load cases that needed to be simulated in order to fulfil AHD's requirements [4]. Table 4.1 enumerates these load cases providing context for the results.

Table 4.1: Load Cases applied to the Boarding Step Models

Load Cases	Value or Description
Weight	Three (3) people of 100 kg standing as illustrated in Figure 2.3
Floats 1	Limit and Ultimate Loads in Direction Z as specified in [4]
Floats 2	Limit and Ultimate Combined Loads in Directions Z, X as specified in [4]
Floats 3	Limit and Ultimate Combined Loads in Directions Z, Y as specified in [4]
Floats 4	Ultimate Load for Ditching Sea State 4 - Up-Load Condition in Direction Z as specified in [4]
Floats 5	Ultimate Combined Load for Ditching Sea State 4 - Drag-Load Condition in Directions Z, X as specified in [4]
Floats 6	Ultimate Combined Load for Ditching Sea State 4 - Side-Load Condition in Directions Z, Y, X as specified in [4]

For the default model, the mesh was assigned generically as mentioned in Section 4.1.1 and refined near the fixture holes to better evaluate stress in those more critical locations. A general view of the mesh is visible in Figure 4.27.

For the removed material model, the mesh was also assigned generically and refined in the same way as the default. However, upon meshing, it was necessary to confirm if the

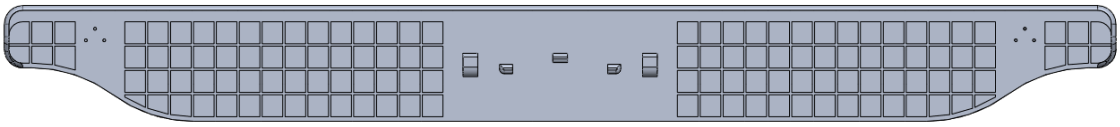

Figure 4.28: Removed Material alternative version

element size was less than half the thickness of the ridges. If the element size were to be more than half the thickness of the ridges, the mesh would not be properly applied and the results accuracy would suffer.

The complex shell model is defined differently. First off, it needs to have its thickness components chosen – that input comes from the analysis made at the end of Section 4.3.4. After being defined for simulation, the mesh can be assigned generically and refined in the same way as the default.

4.3.4 Removed Material and Complex Shell Models

To account for the amount of material that could be removed, a parametric optimization was ran using a matrix of x by y cubes with side l and depth t. The goal was to achieve the lowest mass possible while keeping the deflection under $L/200$ on the Weight load case and the stress under 505 GPa on the Floats 2 Ultimate Combined Loads Load Case (F2U) 4.1. The F2U was selected for the stress constraint because it was the worst case scenario when testing the default model while the Weight load case was selected for the displacement constraint because it is the simulation for the in-use scenario. The dimensions for the sides of the cubes and the thickness of the ridges were based on recommendation by AHD and defined arbitrarily at 45 mm and 5 mm respectively, while the depth was the single variable in the parametric optimization (Figure 4.28). The reason for not including the sides of the cubes or the thickness of the ridges as variables is that when varying their size, the matrix elements' numbers and positions would inevitably have to change. That proved to be a challenge on its own and is something to be tackled in the future simulation and design loops (refer to Chapter 6).

Along the above mentioned, the parametric optimization was ran with the sole goal of minimizing mass. Table 4.2 contains the results of the design study in SW. The results for the δ_{max} are represented in percentage of $L/200$ which is the maximum value admitted for displacement during use. The reason for there only being a value for displacement in the 24 mm column is that the displacement simulation was ran after figuring out the maximum thickness to remove on the stress simulation and the order of simulating backwards, starting at 24 mm and going back until the maximum displacement was lower than $L/200$. In this particular case, the 24 mm value was already under the threshold and so no further simulations were ran.

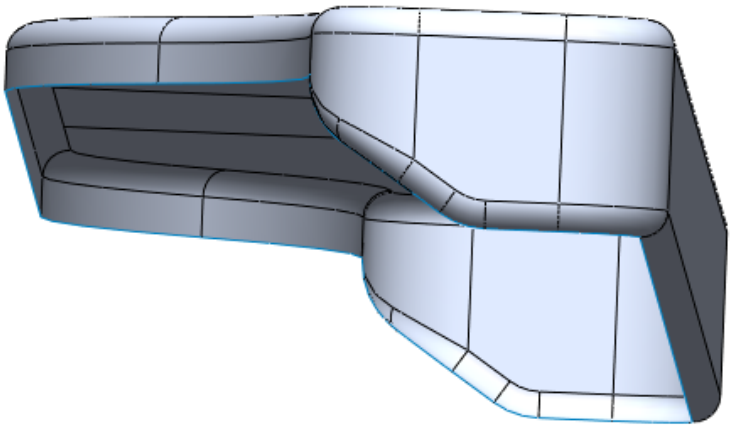

Figure 4.29: Complex Shell Model of the Boarding Step

Table 4.2: Results of the Design Study on the Removed Material for the Boarding Step

Thickness	[mm]	5	7.5	10	12.5	15	17.5	20	22.5	24
F2U σ_{max}	[MPa]	413.1	386.2	403.5	402.8	406.8	407.3	409.2	405.6	393.1
Weight δ_{max}	[%$L/200$]									69.1
Mass	[kg]	38.974	37.158	35.366	33.550	31.735	29.920	28.105	26.290	25.178

As is visible in the table, the removed material model can have nearly all of its thickness removed and still be well below its displacement threshold. Seeing as how removing all the thickness wouldn't be a viable option aesthetically, the final removed material model will have 1 mm, leaving the material removal at 24 mm. This yields $\delta_{max} = 69.1$ % in-use and $m = 25.2$ kg which is a significant reduction of $59,1$ % from the default model's $m = 42.6$ kg.

The complex shell model was obtained by using the Offset Surface tool which allows the user to select the surfaces (or the faces of a solid body) to offset and then set a value for offset distance - which was set to make it so the new shell model was in the middle of the thickness of the solid body model. As it's a surface, this model has no thickness to begin with. Some calculations were made with the intent of figuring out how to correctly input the shell's ply definition in SW. These preliminary calculations used the same simple shell model as the one mentioned in Section 4.3.2 while an equivalent was solved analytically using the Rayleigh-Ritz method.

The relative error between the analytical and FEA values for displacement was less than 1.5 % meaning the shell composite plies are correctly defined and the complex shell model can use the same definition. The complex shell model is visible in Figure 4.29

There were plenty of iterations to figure out the correct amount of plies necessary to have $\delta_{max} \leq L/200$ for the Weight load case since the SW version being used does not yet support including the information on the composite shell definition as variables on a design study.

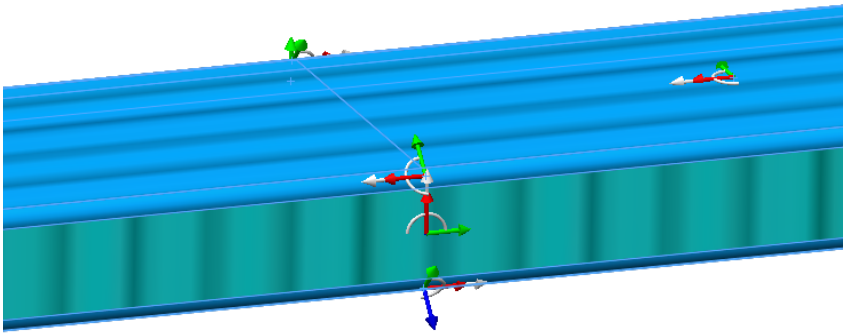

Figure 4.30: Wrong orientation of some of the faces in the model

The initial lay-up was $[0, 90, -45, 45, 0, 90, -45, 45, 0, 90]+[0]+[0, 90, -45, 45, 0, 90, -45, 45, 0, 90]$, where the materials used are Unidirectional Carbon Fibre (CFUD) with an epoxy resin for all layers except the middle one which is an aramid fibre honeycomb. In this lay-up, the CFUD was simulated with 0.15 mm thickness while the honeycomb was set to 10 mm. The lay-up was suggested by AHD and the values for these materials' properties were provided by the company's internal testing results in laboratory.

For the complex shell model from Figure 4.29, the initial lay-up was less than optimal, rendering a FoS of about 0.3 for both the Tsai-Hill and Tsai-Wu criterion around the holes.

However, these results were obtained before the model's faces were correctly oriented. As is visible in Figure 4.30, the highlighted face is, by default, oriented in a way that wouldn't benefit the rigidity of the part. There are several more faces with the wrong orientation which hinder the overall validity of the results unless they're fixed.

By re-orientating all the wrong faces the results improved slightly to a FoS of 0.50 for Tsai-Hill's and 0.53 for Tsai-Wu's criterion. More importantly, the minimum value for these FoS shifted from the edges of the holes to the fillet on the Board Step's depth change (Figure 4.31).

This result led to the assumption that the depth change is hindering the part and so in order to better evaluate the model's options, a simpler U-shape model was created (using the same dimensions for length, hole diameter, width).

This U-shape model (Figure 4.32) yields much better results at a FoS of 0.73 for Tsai-Hill's and 0.69 for Tsai-Wu's criterion. These values are located at the holes as they should be, which might imply that not only is the depth change at fault, but the rear tab's length in the complex model influences results and ought to be increased. By doing so, the rigidity should improve and the FoS values should increase.

Another possible improvement was to add some reinforcements along the direction normal to the longitudinal of the Board Step. These were both introduced to the simulation one at a time (Figure 4.33) and the improvements are substantial as can be seen in Table 4.3

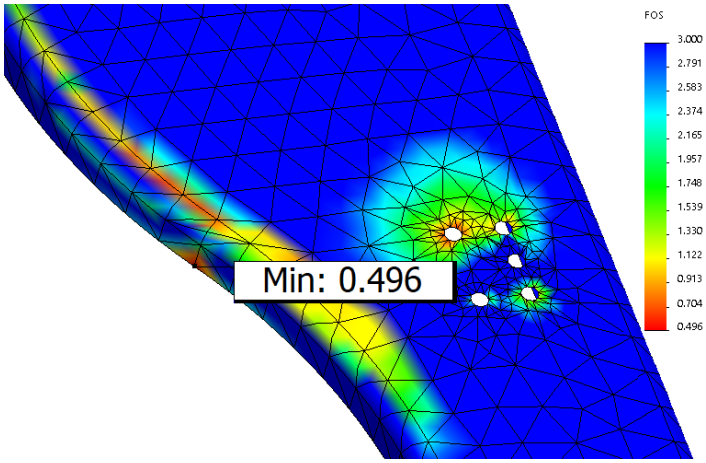

Figure 4.31: Minimum Tsai-Hill value for Complex Shell Model with re-oriented faces

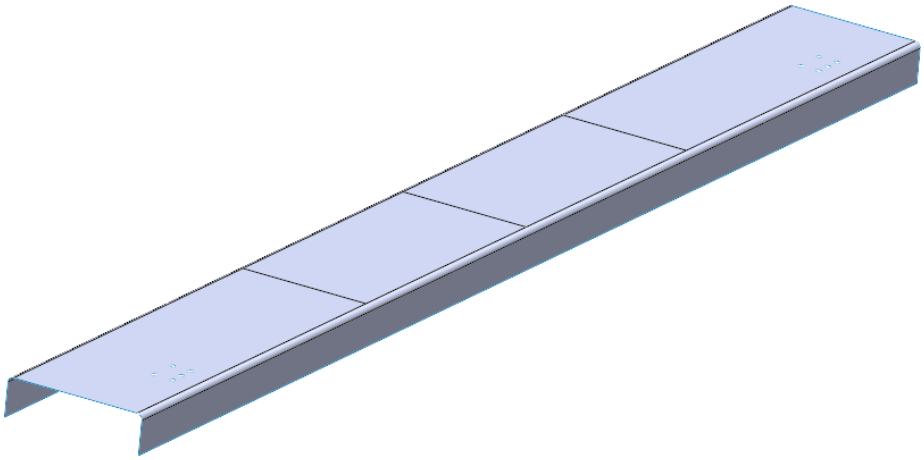

Figure 4.32: U-Shape Shell Model

Table 4.3: Values for the Complex Shell's different Models

Model Designation	Displacement [%L/200]	Tsai-Hill	Tsai-Wu
Initial Lay-Up	554.4	0.289	0.291
Refined Ply Orientation	553.4	0.500	0.530
U-shape Model	208.8	0.731	0.696
Increased Rear Tab (IRT)	227.5	0.588	0.583
IRT and Reinforcements	224.5	0.650	0.646

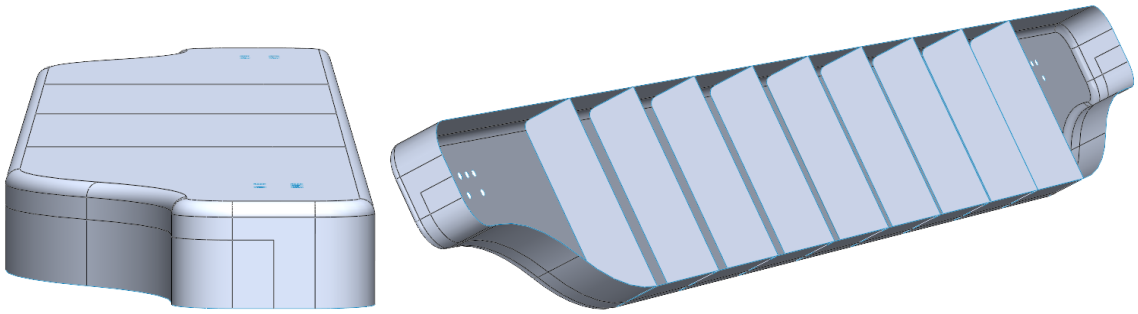

(a) Increased Rear Tab (b) Increased Rear Tab and Reinforcements

Figure 4.33: Improvements on the Complex Shell Model

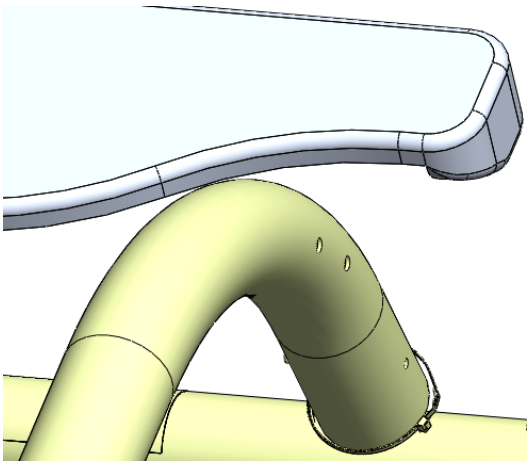

Figure 4.34: Close-up of the Boarding Step and the Landing Gear

The fact that the holes in the Complex Shell model are not centred also originates torsion which may, in conjunction with the lesser depth, be causing the Board Step to fail.

The solution here would be to centre the holes, but that wouldn't be possible using the current model as it would interfere with the depth change which is vital for the step to fit in its allotted space. Figure 4.34 illustrates the reason for this and also why it isn't possible (with the current fixtures configuration) to use the U-Shape model in composite instead.

The U-Shape model would however provide AHD a good basis to improve upon and so in order to validate the model for the Weight simulation its lay-up was was reinforced by adding more plies and increasing the core thickness. The lay-up's ply's orientations are $[0, 90, -45, 45, 0, 90, -45, 45, 0, 90, -45, 45, 0, 90]$+$[0]$+$[0, 90, -45, 45, 0, 90, -45, 45, 0, 90, -45, 45, 0, 90]$ where the outer plies are CFUD at 0.15 mm thickness while the centre honeycomb core was simulated at 20 mm.

In Table 4.4 it's visible that even with a total thickness of 24.35 mm, the composite variant of the Board Step cannot fulfil the rigidity constraint yielding a final displacement of a little over 100 %. Even so, the U-Shape model has a mass of just 7.11 kg making it the

Table 4.4: U-Shape Shell final simulation results

Simulation Designation	Displacement [$\%L/200$]	Tsai-Hill	Tsai-Wu
U-Shape Model Table 4.3	208.8	0.731	0.696
U-Shape Centred Holes (CH)	176.2	0.932	0.848
U-Shape CH 29 Plies (Core 10mm)	137.3	1.299	1.224
U-Shape CH 29 Plies (Core 20mm)	100.1	1.436	1.377

lightest Board Step model in the project.

4.3.5 Simulation Results and Discussion

The default model has the lowest displacement values for all simulations (Figure 4.35) but the highest weight at 42.6 kg.

The removed material model fulfils the displacement constraint in the weight load-case which is the projected in-use scenario while deforming elastically close to 250 % in the F2U load case. This model weights 25.2 kg.

The complex shell model does not fulfil the displacement constraint in its current state. It is suggested that a variant of the u-shape shell model be worked on.

Until a viable composite material version is validated, the removed material model is the best choice to implement. Both solid models fulfil the displacement and stress constraints. Figures 4.35 and 4.36 illustrate a side-by-side comparison for displacement and stress values. It's possible to conclude that by removing material from the underside of the default model, the stress hotspot that exists near the fixtures is alleviated slightly and even though displacement values are on average 2.74 times higher in the removed material model, the utility of the Board Step is not compromised because it never deforms plastically.

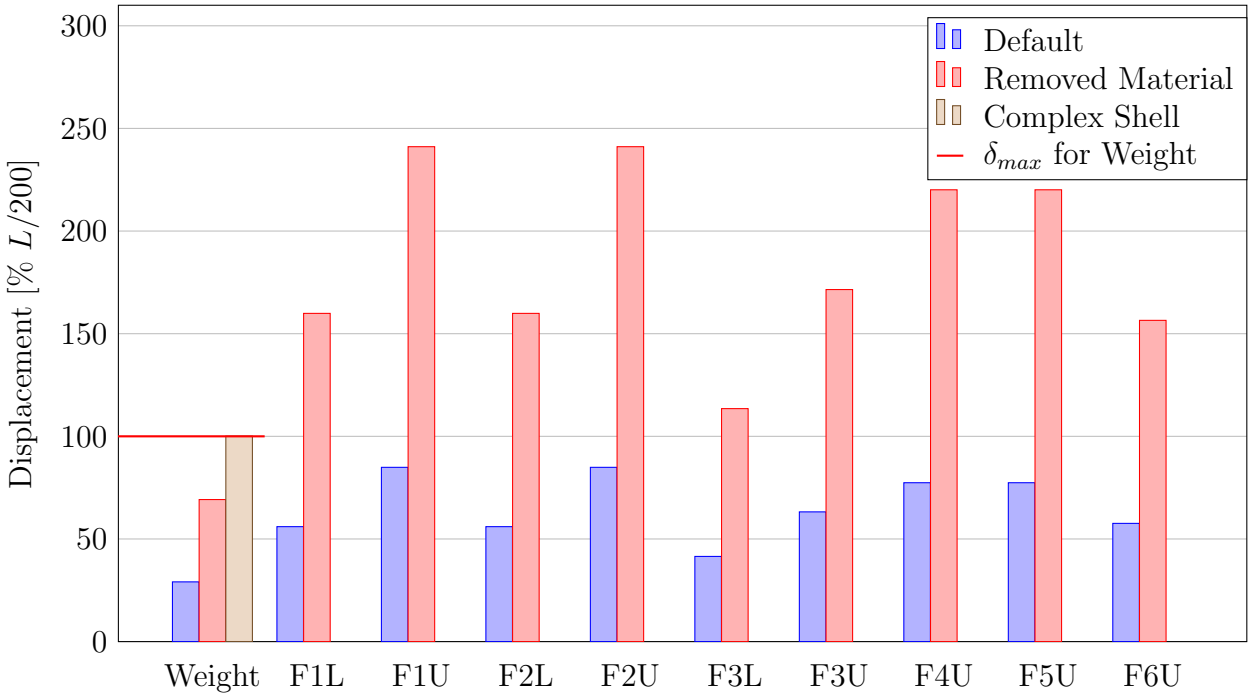

Figure 4.35: Comparison of Displacement Results from all Load Cases in the Different Simulation Configurations

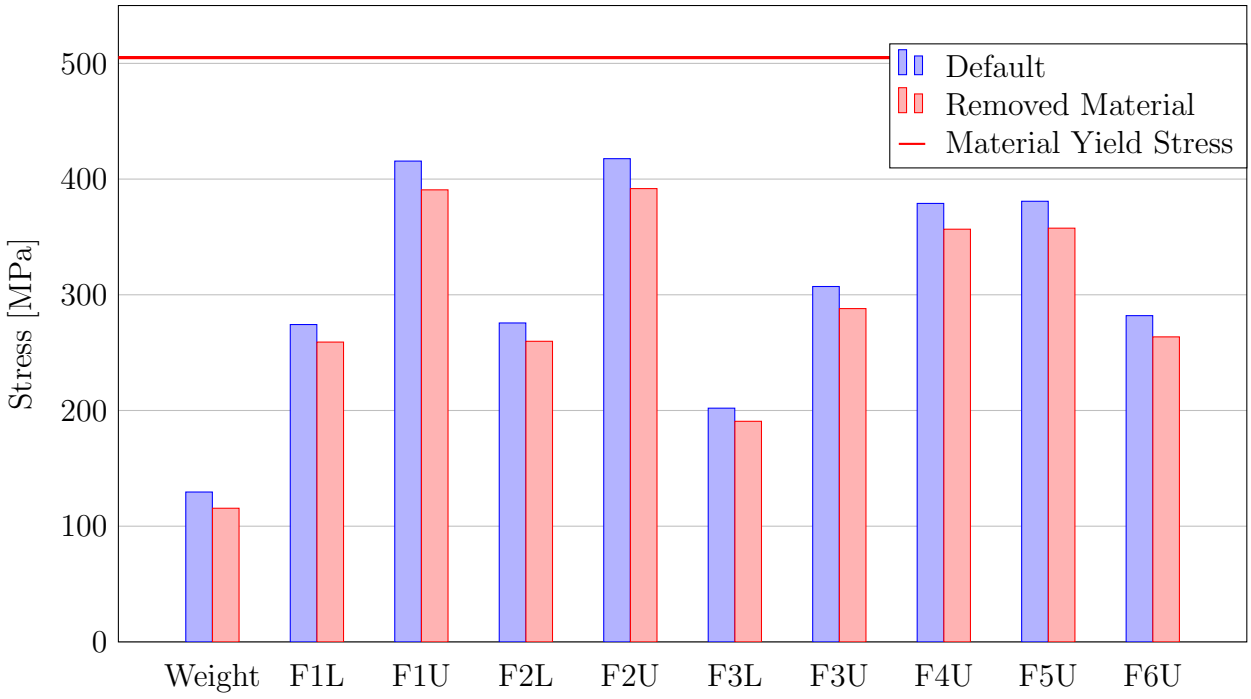

Figure 4.36: Comparison of Stress Results from all Load Cases in the Different Simulation Configurations

Chapter 5

Conclusions

The present work's objective was to provide a worthwhile basis for certification of an equipment in the aeronautical industry. In order to do so, progress followed the same guidelines an industry project would.

As the information regarding the project became clear, the initial sketches were scrapped in lieu of a more complex approach. Throughout the design process, a lot of ideas ended up not being developed and instead passed onto Chapter 6 because they would hinder progress in the remaining planned topics. The final prototype model is visible in Figure 3.12 and at the time contained roughly modelled parts which were improved afterwards.

That prototype was then split into parts which went through stress analysis and re-design loops, during which the constraints enforced by the specifications ([2, 3, 4, 12, 13]) resulted in considerable design changes. Two parametric optimizations were successfully executed managing a significant weight reduction along improved functionality.

The partial composite study on the Board Step allowed some preliminary conclusions on the viability of this part as a composite material. The complete study is suggested in Chapter 6 as a future work.

All in all, the initial objective of submitting a proof of concept is fulfilled and while the final product, visible on the cover of this thesis, is a long way from certification and hence manufacturing, the information throughout the project along with the confidential files and data accessible to AHD render it a good basis to improve upon.

Chapter 6

Future Works

This project is not yet finished. As such, several improvements can be seen in the following sections of this chapter. The next steps towards getting this project to market within the industry would be:

- Weight/Rigidity Optimization loops between the Design and Stress departments;
- Final stress load, performance data, flight characteristics, weight and balance analysis;
- Safety analysis;
- Manufacturability, material, costs, reliability and maintainability analysis;
- Applicability analysis (which aircrafts can this equipment be used in with minimal to no modifications);
- Ground and flight tests and inspections;
- Equipment qualification.

6.1 Composite Boarding Step

As shown throughout Section 4.3.4 the Board Step's composite alternative is viable. The best place to start would be by testing the U-Shape shell model until it fulfils all constraints in the different load cases and then either re-design it to fit the available fixtures in the aircrafts or re-design the fixtures to accommodate the U-Shape shell model.

It would also be necessary to figure out how to insert the biscuits for connecting the Add Step's mechanism as it's an integral part of the overall assembly.

6.2 Increase the Additional Step's Tread

In order to facilitate boarding the steps should be as wide and long as possible (up to the recommended maximum dimensions [16, p. 191-195]). Width is easily achievable but increasing the tread is somewhat more difficult. This idea explores a hinged connection that would extend its tread, effectively doubling it while maintaining its limit dimensions for when not in use (Figure 6.1).

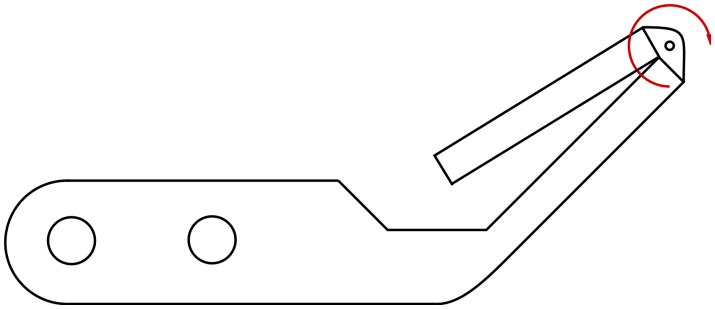

Figure 6.1: Idea to increase tread of the Additional Step by adding a hinged extension

6.3 Choose anti-skid surface for top of steps

It is mentioned in Section 2.3 that it's ideal for climbing steps to have an anti-skid surface on their tread as is illustrated in Figure 2.10. This concept was not researched throughout this project but would be a valuable addition.

6.4 Lock Pin for flight

In Section 3.2's Figure 3.9b is illustrated. The idea behind this locking mechanism would be that a spring-pin or spring-pin-like part would hold the Add Step assembly in place. When pulled, the Add Step would extend towards the users and could easily be locked back in place by pushing it past the pin.

This idea wasn't pursued within the model and as it stands there's some short-comings. These are that a single spring-pin wouldn't be sufficient to eliminate vibration within the assembly while in flight. Another would be the difficult execution of the locking action after all personnel had already boarded the aircraft.

All in all, the concept would have to: be deployable and the assembly locked back into place easily from both inside and outside the aircraft; be designed with the intent of eliminating vibration and hence noise produced by said vibration.

6.5 LED Lamp

When designing for outdoor usage, there should be additional lighting to aid visibility. This was incorporated into the starting design in the form of a yellow indentation visible in Figures 3.3 and 3.12.

6.6 Fatigue Study

All the parts in this project should be subjected to fatigue simulations using their in-use load case as a basis, especially the link parts as they have the lowest safety coefficient.

Bibliography

[1] European Aviation Safety Agency. Explanatory Note to Executive Director Decision 2018/007/R regarding Amendment 5 for Certification Specifications 27 and 29, June 2018.

[2] European Aviation Safety Agency. Acceptable Means of Compliance for Small Rotorcraft CS-27. Certification Specification 5, EASA, June 2018.

[3] European Aviation Safety Agency. Acceptable Means of Compliance for Large Rotorcraft CS-29. Certification Specification 5, EASA, June 2018.

[4] ETVD-097/2018. Requirements Specification for Boarding Step Project. Note, Airbus Helicopters Deutschland GmbH, January 2018.

[5] A. C. Ugural. *Stresses in plates and shells*. McGraw-Hill Ryerson, Limited, 1981. ISBN 978-0-07-065730-4. Google-Books-ID: U71RAAAAMAAJ.

[6] S Timoshenko and S Woinowsky-Krieger. Theory of Plates and Shells. page 591.

[7] Eric Harold Mansfield. *The bending and stretching of plates*. Cambridge University Press, Cambridge [England] ; New York, 2nd ed edition, 1989. ISBN 978-0-521-33304-7.

[8] Solidworks Online Help.

[9] Gouri Dhatt, Emmanuel Lefrançois, and Gilbert Touzot. *Finite Element Method*. John Wiley & Sons, December 2012. ISBN 978-1-118-56970-2.

[10] Klaus-Jürgen Bathe. Finite Element Method. In *Wiley Encyclopedia of Computer Science and Engineering*, pages 1–12. American Cancer Society, June 2008. ISBN 978-0-470-05011-8.

[11] John Edward Akin. *Finite Element Analysis Concepts: Via SolidWorks*. World Scientific Publishing Company, August 2010. ISBN 978-981-310-792-2.

[12] European Committee for Standardization. EN 1993-1-8: Eurocode 3: Design of steel structures - Part 1-8: Design of Joints. Eurocode, CEN, December 2005.

[13] European Committee for Standardization. EN 1999-1-8: Eurocode 9: Design of aluminium structures - Part 1-8: Design of Joints. Eurocode, CEN, December 2005.

[14] Richard Budynas and Keith Nisbett. *Shigley's Mechanical Engineering Design*. McGraw−Hill Series in Mechanical Engineering. McGraw−Hill, 8th ed edition, October 2006. ISBN 0-390-76487-6.

[15] Eastman Kodak Company Staff and The Eastman Kodak Company. *Kodak's Ergonomic Design for People at Work*. John Wiley & Sons, 2004. ISBN 978-0-471-41863-4.

[16] Ernst Neufert and Peter Neufert. *Architects' Data*. Wiley-Blackwell, 4th edition edition, March 2012. ISBN 978-1-4051-9253-8.

[17] Government Publishing Office. Code of Federal Regulations: Title 29 Labor: Subtitle B Regulations Relating to Labor: Chapter Xvii: Part 1910: Subpart D: Section 1910.24. Regulatory information, GPO, July 2010.

[18] Robert M. Thomson, Bernard J. Covner, Herbert H. Jacobs, and Jesse Orlansky. Arrangement of Groups of Men and Machines, Chapter VIII of Human Engineering Guide to Equipment Design. Technical report, DUNLAP AND ASSOCIATES EAST INC NORWALK CT, December 1958.

[19] Koji Murakami, Satoshi Hamai, Ken Okazaki, Hirotaka Gondo, Yifeng Wang, Satoru Ikebe, Hidehiko Higaki, Takeshi Shimoto, Hideki Mizu-uchi, Yukio Akasaki, and Yasuharu Nakashima. Knee kinematics in bi-cruciate stabilized total knee arthroplasty during squatting and stair-climbing activities. *Journal of Orthopaedics*, 15(2):650–654, June 2018. ISSN 0972-978X.

[20] V. S. Rajashekhar, K. Thiruppathi, and R. Senthil. Modelling, Simulation and Control of a Foldable Stair Mechanism with a Linear Actuation Technique. *Procedia Engineering*, 97:1312–1321, January 2014. ISSN 1877-7058.

Appendix A

Planning Proposal

This annex contains the detail of the planning agreement between the student and the advisers (Figure A.1).

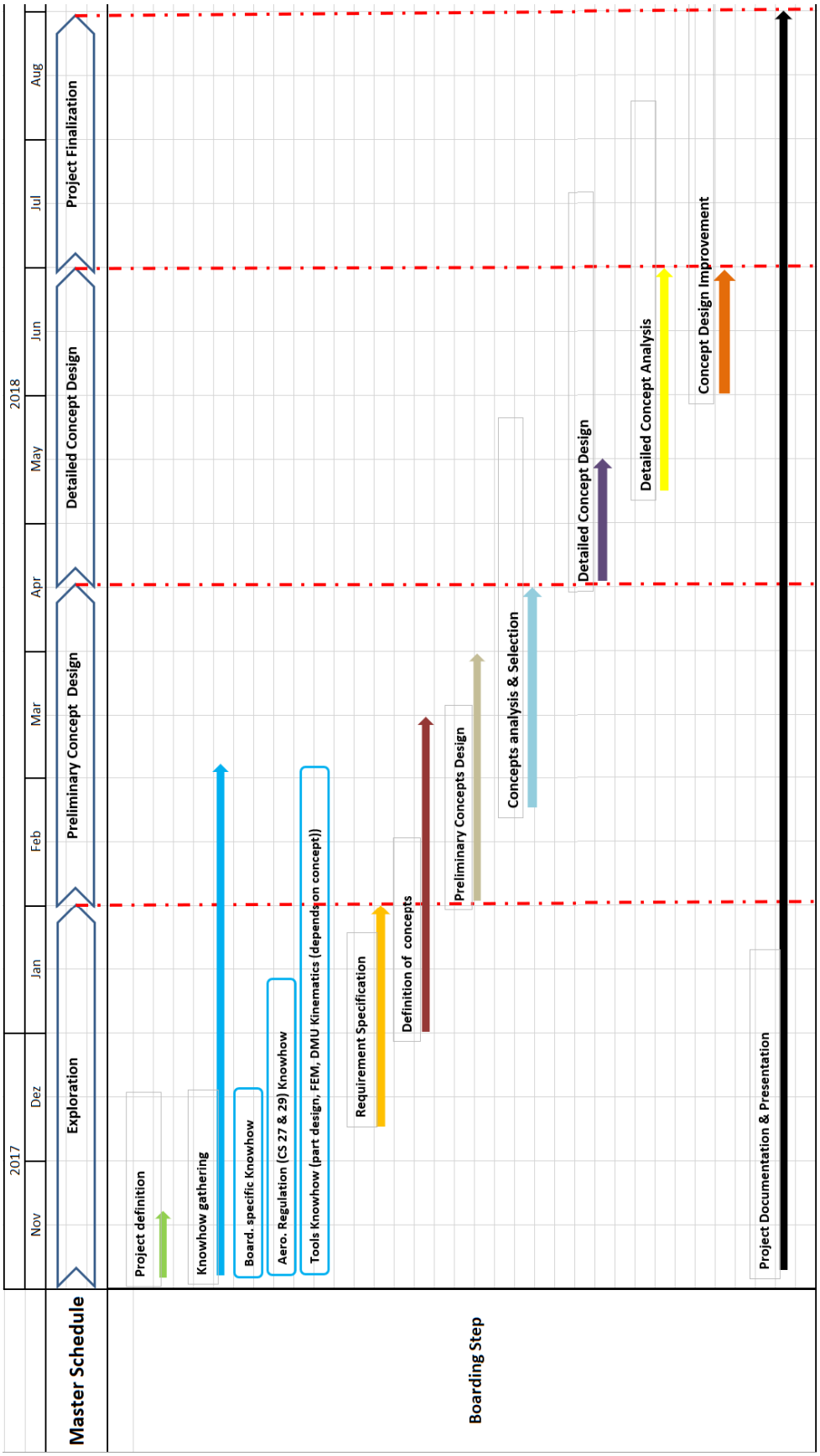

Figure A.1: Schedule breakdown